Protein-protein interactions of the nuclear receptor NR4A2

Tonje Bjørnetrø

Master of Science in Molecular Medicine
Trondheim, Spring 2014

NTNU
Norwegian University of
Science and Technology

Acknowledgement

This thesis is a part of the MSc programme Master of Science in Molecular Medicine at the Faculty of Medicine (DMF), Norwegian University of Science and Technology (NTNU). The work has been performed at the Departmet of Cancer Research and Molecular Medicine (IKM) in the Gastroenterology and Molecular cell biology research group.

First I would like to thank my supervisor, Professor Liv Thommesen for excellent guidance and for sharing her knowledge. I am grateful that you are always positive, enthusiastic and approachable.

I thank my co-supervisor PhD fellow Shalini Rao and senior researcher Kristin Nørsett for teaching me laboratory techniques and always answering all my questions in the lab. I want to thank Lars Hagen and Animesh Sharma at the Proteomics and Metabolomics Core Facility, PROMEC, for Mass Spectrometry analysis, the normalization and statistical work of the data. I would also like to thank my fellow student Guri Solum for help and co-operation, and the rest of the research group for feedback and good working environment.

Finally, I thank Michael Johansen for moral support and proofreading of my thesis.

Abstract

The Gastroenterology and Molecular cell biology research group examines biological mechanisms that are important in the development of gastric cancer. The peptide hormone gastrin is known to play a role in organization and maintenance of the gastric epithelium, however, its role in carcinogenesis is debated. Gastrin induces the expression of the nuclear transcription factor NR4A2. NR4A2 expression has been suggested as prognostic factors and potential therapeutic targets for patients with different cancer types, including gastric cancer. The biological functions of NR4A2 in tumors and the prognostic significance are incomplete and needs to be further studied.

Recent studies indicate that NR4A2 protein-protein interactions as well as its sub-cellular localization are of vital importance when it comes to the specific cellular response. The aim of this study was to characterize interacting partners of NR4A2 in cellular model systems.

In the present study, the expression of the CCK2 receptor and gastrin induced NR4A2 expression in gastric carcinoma cell lines were examined. The MKN45 and HEK293 cells were used to characterize protein-protein interactions of NR4A2. No interactions were observed between NR4A2 and the proteins initially hypothesized to bind to NR4A2. However, Mass Spectrometry in combination with immunoprecipitation identified several potential binding partners. This thesis provides an overview of potential interactions partners of NR4A2 that may be important in gastric cancer and can provide candidate proteins for further work.

Abbreviations

AF-1	Activation function 1
AF-2	Activation function 2
AKT/PKB	Protein kinase B
AMPK	AMP-activated protein kinase
APC	Adenomatous polyposis coli
cAMP	Cyclic adenosine monophosphate
CCK2R	Cholecystokinin 2 receptor
CCKBR	CCK2 receptor gene
COX-2	Cyclooxygenase-2
CREB	cAMP response element-binding protein
DAG	Diacylglycerol
DBD	DNA-binding domain
ECL cells	Enterochromaffin-like cells
FZD10	Frizzled 10
GAST	Gastrin gene
GRP	Gastrin-releasing peptide
GSK3β	Glycogen synthase kinase-3 β
IP	Immunoprecipitation
IP3	Inositol triphosphate
IPA	Ingenuity Pathway Analysis
LBD	Ligand-binding domain
LGR4	Leucine-rich repeat-containing G-protein coupled receptor 4
LPR 5/6	Low-density lipoprotein receptor-related protein 5/6
MACF1	Microtubule-actin cross-linking factor 1
MAPK	Mitogen-activated protein kinase
MS	Mass Spectrometry
MSH6	Mismatch repair protein msh6
NBRE	NGFI-B response element
NR4A	Nuclear receptor subfamily 4, group A
NR4A1	Nuclear receptor subfamily 4, group A, member 1
NR4A2	Nuclear receptor subfamily 4, group A, member 2
NR4A3	Nuclear receptor subfamily 4, group A, member 3
NurRE	Nur-responsive element
OPN	Osteopontin
PAI-1	Plasminogen activator inhibitor 1
PARP-1	Poly (ADP-ribose) polymerase 1
PGE_2	Prostaglandin E_2
PI3K	Phosphoinositide kinase 3
PKA	Protein kinase A
PKC	Protein kinase C
PLC	Phospholipase C
PROMEC	Proteomics and Metabolomics Core Facility, NTNU
RXR	Retinoid X receptor
SERBP1	Plasminogen activator inhibitor 1 RNA- binding protein
SFPQ	Splicing factor, proline- and glutamine-rich

STK11	Serine/threonine-protein kinase STK11
TCF4	T cell factor 4
uPA	Urokinase plasminogen activator

Table of contents

1.0 Introduction

1.1 Gastric cancer

Gastric cancer is a major public health issue. It is the second leading cause of cancer-related death worldwide and the fourth most common cancer type [1]. Overall there has been a downward trend of gastric cancer during the past 70 years; both the mortality and the incidence have fallen dramatically. However, the decline is predominantly caused by the decrease in distal, intestinal type adenocarcinoma, whereas the incidence of proximal, diffuse type adenocarcinoma has been increasing [2]. Gastric cancer is an aggressive disease with a high mortality rate. In Europe, the 5-years survival rate is less than 25% in all gastric cancer patients [3]. Recurrence after curative-intent resection occur in approximately 40-60% of the patients [4].

Gastric cancer is a multifactorial disease and results from a combination of environmental factors and genetic alteration (figure 1.1). Gastric cancer affects mainly older patients that have experienced an extensive period with atrophic gastritis. Gastritis is commonly caused by *Helicobacter pylori* infection and is the single most common cause of gastric cancer [5]. *H. pylori* infection is unlikely to be responsible for gastric cancer development by itself, but might provide an environment leading to carcinogenesis and may impact other environmental exposures and lifestyle. Increased risk of gastric cancer is associated with salty food and N-nitroso compounds and low consumption of fresh fruits and vegetables. Use of tobacco, obesity, pernicious anemia are also thought to increase the risk of gastric cancer [2].

About 90% of gastric cancers are adenocarcinomas, where the cancer develops from cells of the innermost lining of the stomach [2]. Two histological types of adenocarcinoma are characterized, diffuse and intestinal. These two types show different epidemiological and pathological features. The diffuse type is more frequent in young patients, can be multifocal and hereditary. It generally evolves after chronic inflammation without passing through the intermediate steps of atropic gastritis or intestinal metaplasia (figure 1.1) [5]. Intestinal type occur more commonly in older

patients, and are often related to environmental factors such as *H. pylori* infection, diet and lifestyle [6]. The development follows multifocal atropic gastritis, accompanied by intestinal metaplasia and leads to cancer through dysplasia (figure 1.1) [5].

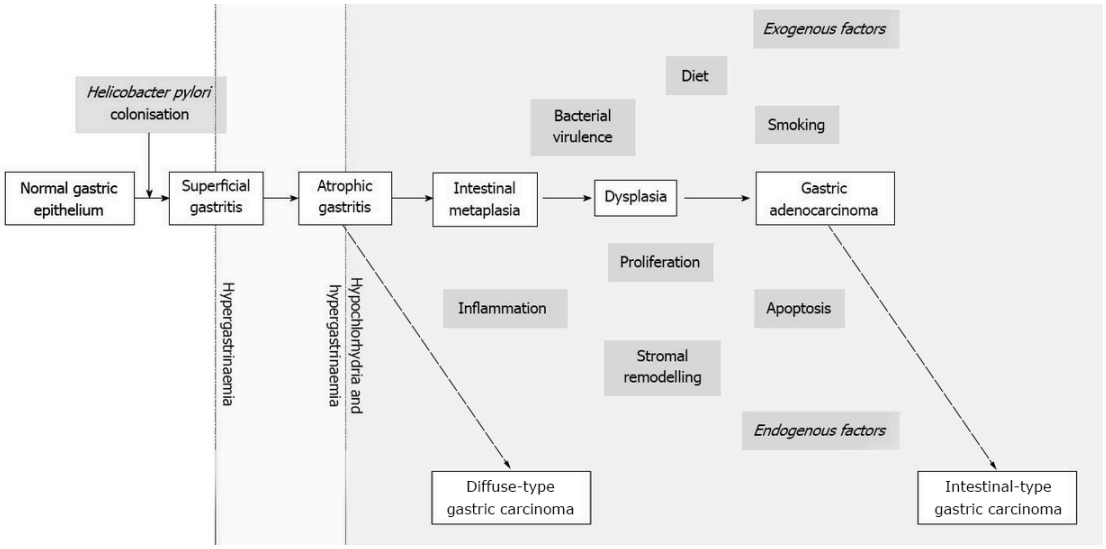

Figure 1.1. Schematic representation of the development of gastric cancer. Development of intestinal type of gastric cancer follows a characteristic pathological pathway, comprising progression from atrophic gastritis, via metaplastic to dysplasia and malignancy. Diffuse type of gastric cancer develops from normal gastric epithelium, generally after chronic inflammation **(Modified from Burkitt *et al.* [7]).**

During gastric carcinogenesis an accumulation of genetic abnormalities occurs and some variations have been reported to increase the risk of developing gastric cancer. Oncogenic activation and tumor-suppressor gene inactivation plays crucial roles in the process of tumorigenesis and cellular immortalization. Other important factors are inactivation of DNA repair genes and cell adhesion proteins, overexpression of growth receptors and growth factors [6, 8].

1.2 Gastrin

The polypeptide hormone gastrin is important in regulating gastric acid secretion [9]. Gastrin has been shown to have an important role in maintaining functional integrity of the gastric epithelium and is also known to stimulate gastric mucosal growth [10]. The gastrin gene (*GAST*) encodes a 101 amino acid polypeptide, preprogastrin. After synthesis of preprogastrin, the gene products are prone to different posttranslational

modifications that result in different biologically active peptides. Gastrin- 17 is the predominated form secreted in the human stomach [7]. In addition, gastrin is also expressed in the colon, fatal islets in pancreas, pituitary and spermatozoa but in lower levels [11]. In the mature form, gastrin interacts with the G protein-coupled receptor cholecystokinin 2 (CCK2) receptor [12]. The CCK2 receptors are located on several cell types in the central nervous system and peripheral organs including the stomach. In the gastric epithelium, it is primarily the parietal cells and enterochromaffin-like (ECL) cells that possess the CCK2 receptor [10].

1.2.1 Acid secretion

The main function of gastrin is to regulate gastric acid (HCl) secretion in the gastric mucosa to maintain the appropriate acidic pH for the digestive enzymes [13]. Gastrin is synthesized and secreted by G cells located in the gastric antrum of the stomach (figure 1.2) [12]. The G cells respond to a number of luminal stimuli including amino acids and dietary amines [7]. Subsequently, gastrin is transported to the oxyntic mucosa in an endocrine manner and interacts with gastrin receptors on ECL cells and potentiates the release of histamine. An increase in histamine concentration induces gastric acid secretion by parietal cells [13]. Gastrin secretion is tightly regulated by gastrin-releasing peptide (GRP) and somatostatin as a positive and a negative regulator, respectively, to facilitate the release of gastric acid from parietal cells [13].

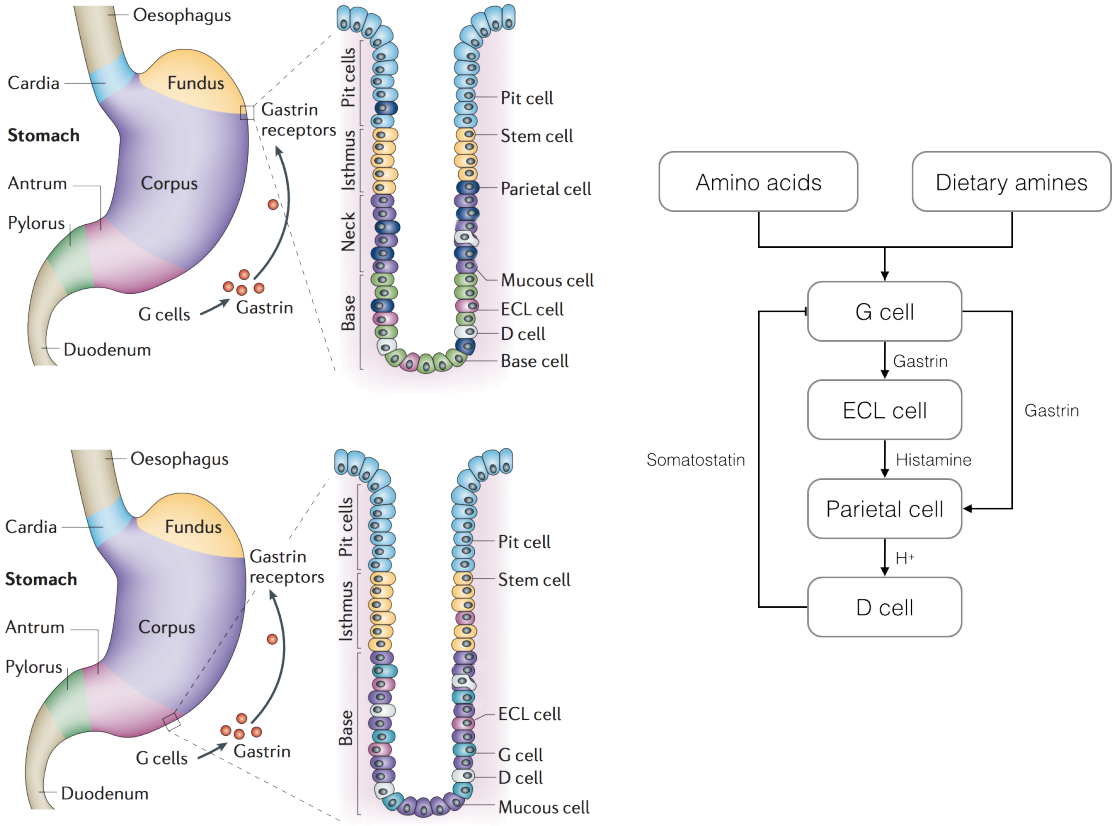

Figure 1.2. The role of gastrin in acid secretion regulation. The upper part of the stomach consisting of cardia, fundus and corpus and is involved in acid secretion. The lower part, antrum and pylorus, are the main site for gastrin synthesis in the G-cells. Gastrin is secreted and enters the circulation and act on the CCK2 receptors at the ECL cells. Upon gastrin stimulation the ECL cells release histamine that act on parietal cells and stimulating them to secret gastric acid. Gastrin secretion is regulated by the two proteins somatostatin and gastrin-releasing peptide (**Modified from Watson *et al.* [13] and Burkitt *et al.* [7]).**

1.2.2 Homeostasis of gastric mucosa

The gastric epithelium is folded into tubular branched gastric glands that reach deep into the muscularis mucosa (figure 1.2). Pluripotent stem cells are located in the isthmus or neck region of the gastric gland. These cells proliferate, migrate up or down and differentiate and ultimately give rise to all cells of the gastric epithelium [10, 14].

Knock-out studies for the gastrin gene (*GAST*) or CCK2 receptor gene (*CCKBR*) has confirmed that gastrin has a pivotal role in organization and maintenance of the gastric epithelium, as it regulates proliferation, migration and differentiation of cells

[10, 15-17]. Chen *et al.* [18] studied the morphology and function of ECL cells in CCK2 receptor- deficient mice and showed that the hypergastrinemic response is ineffective because of the target receptor is absent and thus preventing the receptor-signalling cascade. Knock-down of the receptor resulted in thinner oxyntic mucosa, absence of normal ECL cells and a reduction in parietal cells and impaired acid secretion. In the gastrin-deficient mice, Friis-Hansen *et al.* [16] found that the parietal cells was decreased in number and appeared to be immature and had reduced ability to secrete acid. In the same study they found that the acid secretion could be partly restored after 6 days of gastrin administration, and the number of mature parietal cells increased.

Long-lasting conditions of hypergastrinemia has been shown to promote gastric adenocarcinoma in mice and the development of ECL cell hyperplasia and ultimately malignant carcinoids tumors [13]. In the transgenic mouse model INS-GAS, the gastrin expression is targeted to pancreatic β-cells. Initially these mice showed mild hypergastrinemia and increased proliferation in the gastric mucosa. Parietal cells increased in number and enhanced secretion of gastric acid. After 4 months, the parietal cells and acid secretion was lost and the mice developed hyperplasia. Older INS-GAS mice were predisposed to develop gastric cancer and infection with *Helicobacter felis* accelerates this development [19].

Hypergastrinemia and ECL cell carcinoids occur in humans with gastrin-secreting tumors (gastrinomas) and atrophic gastritis/or pernicious anaemia [20]. In atrophic gastritis there is a loss of parietal cells, which leads to loss of acid secretion, and consequently disrupting the normal inhibition of the G-cells. 30% of patients with gastrinoma and 5% of patients with gastritis or pernicious anaemia develops ECL cell carcinoids [20].

1.3 Gastrin and gastrointestinal cancer

Since the mid-1980s, there has been an increasing interest in research of the role of gastrin in carcinogenesis [13]. Gastrin has been shown to be a growth factor in malignancies of the gastrointestinal tract, medullary thyroid cancer, and small lung cancer as well as tumors of the central and peripheral nervous system [17, 21].

Henwood *et al.* [22] studied the expression of gastrin and the CCK2 receptor in a stepwise progression monitoring premalignant changes within the gastric mucosa. Human tissue samples from patients showed an increased expression of both gastrin and the CCK2 receptor in atrophic gastritis to intestinal metaplasia, dysplasia, and gastric adenocarcinoma. The expression level of the receptor increased significantly from atropic gastritis to gastric adenocarcinoma with a median increase from approximately 5% to 34% of the tissue area [22]. In another study on gastric adenocarcinoma patients found gastrin and its receptor to be significantly related. The expression level of gastrin and the receptor was high in gastric adenocarcinoma tissue of patients, with approximately 48% gastrin positive and 57% CCK2 receptor positive tissue samples [23]. In the same study, gastrin and CCK2 receptor expression were not found to be significant prognostic factors, however the prognosis of patients positive for both gastrin and CCK2 receptor were significantly poorer than for those negative for gastrin and CCK2 receptor in diffuse-type gastric cancer patients. These results indicate that for this subgroup of gastric carcinoma, gastrin has a role as an autocrine growth factor [23]. Somatic mutations in CCK2 receptor gene have been identified in colorectal and gastric tumors and the changes affect cellular behaviour and promote tumor progression [24].

Gastrin might influence carcinogenesis through several signalling pathways. It mediates gene expression associated with cell division, invasion, angiogenesis and anti-apoptotic activity (figure 1.3) [13]. Gastrin binds to the CCK2 receptor and signalling via the Gq_{11}- protein to activate several secondary messengers. At an early stage, activation of phospholipase C (PLC) results in the production of the secondary messengers inositol triphosphate (IP3) and diacylglycerol (DAG). These events result in intracellular Ca^{2+} release and activation of protein kinase C (PKC) [17]. Upon activation of CCK2 receptor through PKC-dependent mechanisms, the mitogen-activated protein kinase (MAPK) pathways are activated [12]. MAPK pathways are central in regulating cell proliferation and migration in a gastrin mediated manner [12]. The phosphoinositide kinase 3 (PI3K) pathway, is involved in gastrin dependent cell proliferation and anti-apoptotic action of the CCK2 receptor, as well as regulation of migration and cell adhesion [12]. All together, these signalling pathways are important in carcinogenesis and associated with tumor progression and cell survival [12, 17, 25].

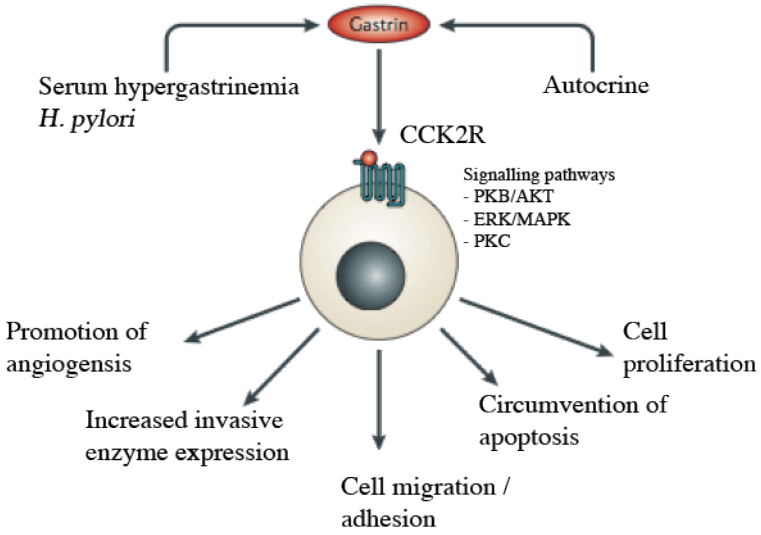

Figure 1.3. Gastrin mediates gene expression associated with a myriad of cellular functions. Upon activation of the CCK2R, several the signalling pathways are activated and that can influence the carcinogenesis (**Modified from Watson *et al.* [13]).**

Several hundreds genes not known to be regulated by gastrin were identified by Selvik *at al.* [26] in our group as gastrin responsive genes in the pancreatic adenocarcinoma cell line AR42J. In this study it was found that gastrin treatment seemed to activate genes involved in ER stress/survival. These findings may improve the understanding of how gastrin affects pathophysiological processes [26]. NR4A2 was one of the genes found to be a gastrin responsive gene, and thus became of interest to this group.

1.4 NR4A2

Nuclear receptor subfamily 4, group A, member 2 (NR4A2) is a transcription factor belonging to the orphan nuclear receptor family NR4A [27]. Receptor knock-down or overexpression *in vivo* and *in vitro* has demonstrated pro-oncogenic or suppressor-like activity of orphan receptors [28]. During the last couple of years, NR4A2 expression has been suggested as prognostic/predictive factors and potential therapeutic targets for patients with different cancer types including gastric cancer, colon cancer, bladder cancer, prostate cancer and breast cancer [28-34]. The biological functions of orphan nuclear receptors in tumors and the prognostic significance are incomplete and needs to be further studied.

The NR4A subgroup includes NR4A1 (Nur77), NR4A2 (Nurr1) and NR4A3 (Nor1). The NR4A nuclear receptors are expressed in skeletal muscle, adipose, heart, kidney, T-cells, liver and the brain [27, 35] and are important regulators of proliferation, apoptosis and differentiation [35]. The NR4As is involved in processes including cardiovascular disease, apoptosis, neurological disease, steroidogenesis, inflammation, metabolic disease and oncogenesis [36].

Nuclear receptors activates or repress target genes by binding directly to DNA response elements or by binding to other transcription factors [37]. NR4A2 binds to target genes either as a monomer, homodimer or heterodimer with e.g. retinoid X receptor (RXR) (figure 1.4). As a monomer the DNA binding site for all the three NR4A receptors is the NGFI-B response element (NBRE). As homodimers and heterodimers with other NR4A members, they bind to the Nur-responsive element (NurRE). NR4A1 and NR4A2 can in addition bind as a heterodimer with e.g. RXR receptor to the DR5 motif [38].

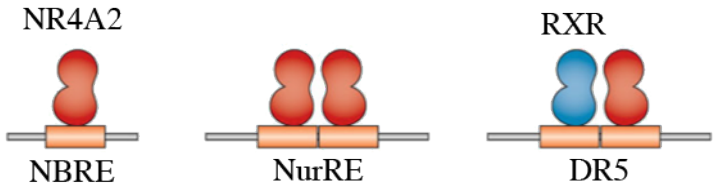

Figure 1.4. DNA response elements recognized by NR4A2. NR4A2 is a transcription factor binding either as a monomer, homodimer or heterodimer with e.g. RXR to different DNA response elements **(Modified from Decressac *et al.* [39])**

The structural organization of the NR4As reveals that the three receptors have well-conserved homologous DNA binding site (91-95%) and C-terminal ligand binding domain (60%), but a highly variable N-terminal (figure 1.5) [38].

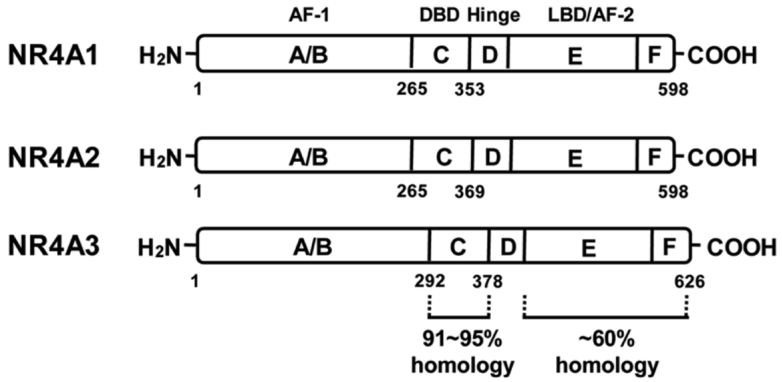

Figure 1.5. NR4A have a common structural organization of their functional domains. The nuclear receptors compose of an amino-terminal activation domain AF-1, a DNA-binding domain (DBD) separated by a hinge region, and ligand-binding domain (LBD) with a short conserved helical sequence referred to as activation function 2 (AF-2) at the carboxyl-terminal end of the LBD [40] **(From Safe *et al.* [38])**

The NR4A2 ligand-binding domain (LBD) is folded in a way that resembles an agonist-bound, transcriptionally active LBD in nuclear receptors. X-ray crystal structure analysis of the LBD displays that NR4A2 does not have a typical ligand-binding cavity, instead this space is occupied by tightly packed, bulky hydrophobic amino acid residue side chains. As these amino acids are conserved in this subfamily, it is predicted that all the members are ligand-independent transcription factors [41]. It has been shown by mutation analysis that the activity of the three receptors is independent of the LBD [35].

A coactivator hydrophobic binding cleft is normally found in nuclear receptors, but in NR4A2 this interacting surface is significantly different. These findings indicate that NR4A2 is incapable to interact with a coactivator or a corepressor through the classical coactivator site of nuclear receptors [41]. Consequently, the transcriptional activity of these receptors is primarily dependent on the level of expression and posttranslational modifications [35]. Activation or deactivation of nuclear NR4A depends on posttranslational protein modifications such as phosphorylation, acetylation, ubiquitination and sumoylation that facilitate the recruitment of coactivators or corepressors [38]. NR4A2 is primarily phosphorylated by MAPK or AKT, and sumoylated by protein inhibitor of activated STAT-γ [42-44]. Several recent described agonists interacts with these receptors either by modulating the N-terminal AF-1 domain or the C-terminal LBD [36].

Another important regulatory mechanism for transcriptional activity of the nuclear receptors is their subcellular localization and dynamic movement. Nuclear receptors and their co-regulators are known to translocate between the nucleus and the cytoplasm, thus the level of expression and the concentrations of the co-regulators gives an additional level of regulation [45]. The shuttling of NR4A2 in and out of the nucleus is regulated by a nuclear localization signal (NLS) within the DNA binding domain and two nuclear export signals (NES) in the ligand-binding domain. Upon oxidative stress, NR4A2 was distributed and found to accumulate in the cytosol thus reduceing expression of NR4A2-dependent genes and loss of phenotype of the dopaminergic cell line MN9D [46].

1.5 The role of NR4A2 in cancer

The NR4A subgroup are immediate early response genes that are induced by a various range of physiological and physical stimuli [27]. These include prostaglandins, fatty acids, growth factors, neurotransmitters, hormonally-active peptides, and other cellular stressors such as fluid sheer stress, and membrane depolarization [38]. NR4A2 emerges as an important regulatory node in biological networks and is characterized as a hub gene. Activation of NR4A receptors is regulated by several kinase pathways and they have been recognized as molecular switches in apoptosis, DNA-repair, proliferation, migration, inflammation, metabolism and angiogenesis, altogether being processes associated with carcinogenesis (figure 1.6) [47].

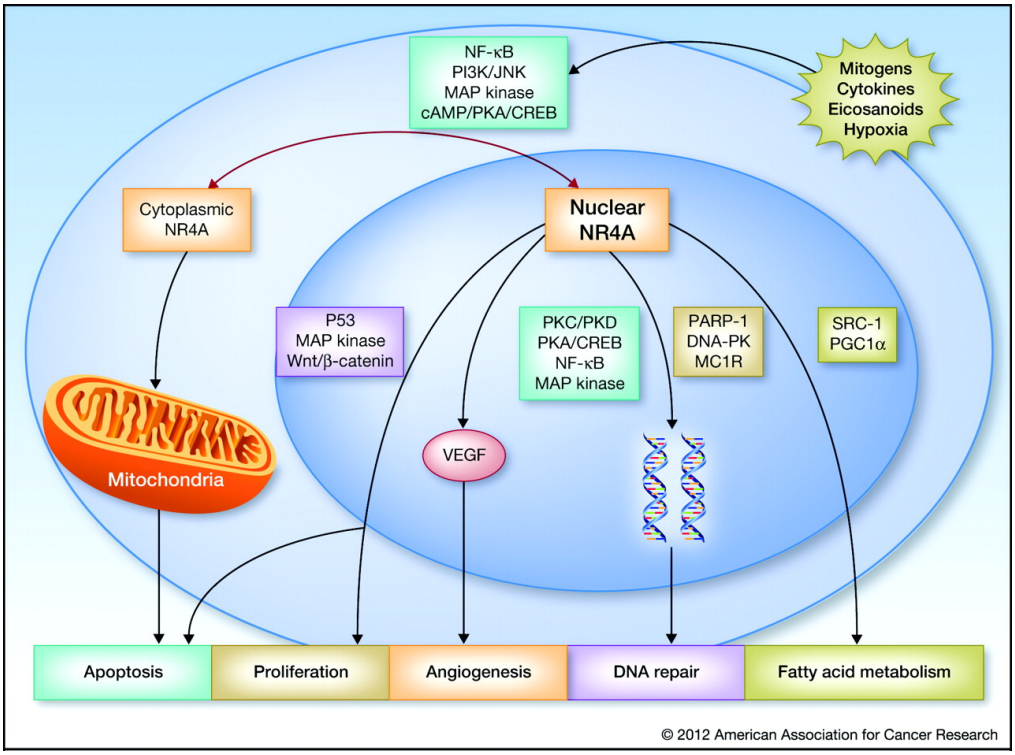

Figure 1.6. The NR4A receptors are involved in various cellular functions that are important in carcinogenesis. A various range of stimuli activate the NR4A receptors, and upon activation they act as transcription factors and alter the expression of downstream genes modulated by multiple signalling pathways. Apoptosis, proliferation, angiogenesis, DNA repair and fatty acid metabolism are all important features in cancer and during cellular stress **(From Mohan *et al.* [47]).**

It has been found that orphan transcription factors may serve as both positive and negative prognostic factor depending on the cancer type. Overall, the NR4A2 receptor seems to exhibit oncogenic activity in most cancer types, but functional and prognostic studies are limited and needs to be further studied [28]. Inamoto *et al.* [30] investigated the clinicopathologic relevance of NR4A2 in a cohort of bladder cancer patients. They found that NR4A2 expression was higher in cancer patients compared to healthy controls. Higher levels of cytoplasmic NR4A2 correlated with distant metastasis and lower patient survival. They also found that increased expression of NR4A2 in tumor cells correlated with increased tumor stage and an invasive growth pattern [30]. In breast cancer etiology, the NR4A2 receptors appear to have a dichotomous role. NR4A2 is higher expressed in normal breast epithelium compared to breast cancer tissue, and therefore loss of NR4A2 expression is associated with oncogenic transformation of the breast epithelium. In the same study, they found that breast cancer patients with lymph node metastasis had a lower NR4A2 expression. Contradictory, NR4A2 silenced breast xenografts showed a significant decreased

growth compared to the control [32]. This suggests that its role may be impacted by the cellular context and stage of carcinogenesis and specific protein-protein interactions in its role in mediating malignancies [32].

Recent studies show that NR4A2 expression predicts poor prognosis and drug resistance in colon and gastric cancer [29, 34]. NR4A2 expression predicted an unfavourable prognosis, especially for those who received chemotherapy, after curative surgery of patients with gastric cancer. This study indicate that NR4A2 might serve as a prognostic and predictive factor for patients with gastric cancer [29]. NR4A2 appears as an important factor linking inflammation and cancer [33, 47]. Aberrant expression of NR4A2 activates several signalling pathways related to inflammation and promotes the development and progression of gastrointestinal cancers [33]. Cyclooxygenase-2 (COX-2) is up-regulated in inflammation and cancer, and induces the production of pro-inflammatory prostaglandin E_2 (PGE_2) [33]. In colorectal cancer, NR4A2 is up-regulated *in vivo* and *in vitro* upon PGE_2 treatment in a cyclic adenosine monophosphate (cAMP)/protein kinase A (PKA)-dependent manner, and contribute to the survival of colorectal cancer cell by inhibiting apoptosis [48]. It has also been shown in colorectal cancer that NR4A2 activates the promoter of osteopontin (OPN). OPN is a direct target of the Wnt-signalling pathway and is known to promote tumor progression and is involved in processes like invasion, metastasis and angiogenesis in colorectal cancer [29, 49]. Blocking of the NR4A2 and the Wnt-signalling pathway appear to be involved in the anti-tumor activity of COX-2 inhibitors [49].

NR4A2 has been characterized as a hub gene associated with liver metastasis, and suggested as a tumor suppressor in gastric cancer. Both the transcriptional and translational level of NR4A2 was significantly down-regulated in liver metastasis compared to the paired primary tumor [50]. In our group, experiments performed by Misund *et al.* [51] found that gastrin induced NR4A2 gene expression in a PKA and PKC dependent manner in the gastric adenocarcinoma cell line AGS-G_R. Endogenous NR4A2 was also observed *in vivo* in normal gastric mucosa in the ECL cells. Since the ECL cells possess the CCK2 receptor this further confirms that NR4A2 expression is activated by gastrin [51]. In the same study, knock-down experiments with siRNA targeting NR4A2 increased migration of gastrin treated adenocarcinoma

cell, while ectopically expressed NR4A2 increased apoptosis and hampered gastrin induced invasion, indicating a tumor suppressor function of NR4A2. Gastrin also affected the nucleus-cytosol shuttling of NR4A2 in these cells, higher amounts of NR4A2 were localized to cytoplasm upon gastrin stimulation [51]. Therefore it is of interest to find protein-interacting partners of NR4A2 in gastric adenocarcinoma cells.

1.6 Aim of the study

The transcription factor NR4A2 has been reported to play an ambiguous role in carcinogenesis. Recent studies indicate that NR4A2 protein-protein interactions and sub-cellular localization of NR4A2 are of vital importance when it comes to specific cellular responses. Gastrin has been shown to induce the expression of NR4A2 and also modifies its nucleus-cytosol shuttling in the gastric adenocarcinoma cell line AGS-G_R.

The overall aim of this study was to characterize protein-binding partners of NR4A2. We hypothesized that gastrin stimulation would affect the binding partners of NR4A2, and thus examined gastrin treated MKN45 cells. The HEK293 cells were included as a non-gastric-cancer cell line.

The aim of the study was:

- Characterize the NR4A2 expression and CCK2 receptor expression in gastric cancer cell lines to further establish a cell line model that could be used to elucidate the role of gastrin-mediated NR4A2 expression and function
- Establish transient transfection of NR4A2 in appropriate cell lines
- Examine NR4A2 bindings partners by immunoprecipitation (IP) and Western blot
- Utilize a proteomic approach with Mass Spectrometry on the IP samples to characterize protein-protein interactions
- Validate the proteins by IP and Western blot

2. Material and methods

2.1 Cell lines and reagents

Cells were incubated in a humidified environment of 5% pCO_2 and at 37°C. The growth medium was added 100 U/ml penicillin, 100 µg/ml streptomycine and 1 µg/ml Fungizone (all from Gibco, Life Technologies).

The human cell line KATO-III cells is derived from signet-ring cells of gastric carcinoma and was purchased from American Type Culture Collection (ATCC) and grown in RPMI-1640 medium (Sigma) with 20% fetal calf serum (FCS) (Sigma). HEK293 cells (ATCC) are derived from human embryonic kidney. The MKN45 cells are derived from a poorly differentiated adenocarcinoma of the stomach, provided from Prof. Sue Watson (Department of Surgery Queens Medical Centre University Hospital Nottingham, UK). HEK293 cells and MKN45 cells were both grown in Dulbecco's Modified Eagle Medium (DMEM) (Gibco) with 10% FCS.

pEGFP-NR4A2 (appendix 1) and pEGFP plasmids were kindly provided by BSc Kevin McMahon, University Collage Dublin, Ireland. The NR4A2-pCMX and pCMX plasmids were a gift from Prof. Thomas Perlmann, Karolinska Institute, Sweden.

Gastrin (G-17) was purchased from Sigma-Aldrich.

2.2 Seeding of cells

The medium was removed and the cells were washed with 0.25% trypsin with EDTA (Gibco), and subsequently incubated with trypsin at 37°C. To deactivate the trypsin, growth medium with FCS was added. The cells were then collected and centrifuged (120x g, 8 minutes) and the cell pellet further dissolved in 10 ml of media. Table 2.1 gives an overview of the number of cells seeded in the different plates.

Table 2.1. Number of cells seeded.

Cell line	Number of cells			
	96 well plate	**6 well plate**	**100 mm^2 petri dish**	**Lab-Tek 8 well**
MKN45	0.01x 10^6	0.3-0.4x 10^6	1.5x 10^6	0.05x 10^6
HEK293	0.02x 10^6	0.3x 10^6	2.0x 10^6	
KATO-III		0.45x 10^6		

2.3 Purification of EGFP-NR4A2 plasmid

EGFP-NR4A2 plasmids were kept in a glycerol stock at -80°C. A small amount of the bacteria in the glycerol stock was picked (using a pipette tip), inoculated in 3 ml LB broth containing 30µg/µl kanamycin (Sigma) and incubated with vigorous shaking (37°C, over night). The Qiagen Plasmid Maxi Kit (Qiagen) was used to purify the plasmids. The protocol from the manufacturer was followed.

The DNA concentration was measured by Nanodrop spectrophotometer (Thermo Scientific) at 260 nm.

2.4 Transfection of cells

The cells were seeded in six-well plates or 100mm^2 petri dishes according to table 2.1, and incubated for 24-48 hours. To transfect cells, different amount of DNA and Metafectene PRO (Biontex) were used for the various cell lines (table 2.2). Plasmids and Metafectene PRO were diluted in growth medium without serum, mixed together and incubated at room temperature (15-20 minutes) before added to the cells. After 4-6 hours the medium was replaced with medium with or without serum. 24-48 hours post transfection the transfection efficiency was assessed using IX71 inverted microscope (Olympus).

Table 2.2. The transfection protocol used for MKN45 and HEK293 cells.

	6 well plate			100 mm^2 petri dish		
	DNA (µg)	Metafectene PRO (µl)	Transfection efficiency	DNA (µg)	Metafectene PRO (µl)	Transfection efficiency
MKN45						
pEGFP-NR4A2	2.5	7	50%	20,0	60,0	50-60%
pGFP	2.5	7	60%	20,0	60,0	50-60 %
pCMX	2.5	7				
HEK293						
A. pEGFP-NR4A2	2.0	4.0	70%	13.0	40.0	90%
B. pEGFP-NR4A2	2.5	6.0	80%			
C. pEGFP-NR4A2	3.0	9.0	80%			
D. pEGFP-NR4A2	3.5	10.5	80%			
pEGFP	2.5	6.0	90%	13.0	40.0	90%

2.5 Western blot

The cells were serum-starved before treated with 10 nM gastrin. The medium was then removed and the cells were washed and incubated with trypsin. To deactivate the trypsin, cold PBS (Thermo Scientific) with 10% FCS was added. The cells were harvested and centrifuged (430x g, 8 minutes). The cell pellet was resuspended in 1 ml PBS with 10% FCS and centrifuged at 4°C (430x g, 8 minutes). Further, the cells were lysed in Urea lysis-buffer ((8M Urea (Sigma), 0.50% Triton x100 (VWR), 0.1 M DTT (Sigma Aldrich), protease inhibitor cocktails 1x Complete (PI) (Roche), 5x PIC2 (Sigma), 5x PIC3 (Sigma)) by adding 2x the volume of the cell pellet, vortexed (30 seconds multiple times), and subsequently centrifuged at 4°C (16 000x g, 16 minutes).

Bio-Rad Protein Assay Dye Reagent Concentrate (BioRad Laboratories) was used to estimate the protein concentration of the samples. 1 µl of the sample was diluted in 1 ml of Bio-Rad solution (diluted 1:5 in H_2O) and vortexed. The absorbance was measured at 595 nm (Shimadzu Spectrophotometer). To determine the protein concentration the mean absorbance value of three replicates were calculated from a standard curve generated in Bovine serum albumin (BSA) (Sigma). The samples were then stored at – 80°C.

When running the gel; protein samples (amount provided in table 2.3) were mixed with NuPAGE LDS Sample Buffer (Invitrogen Life Technologies) and diluted with dH_2O to obtain equal volume of the samples and subsequently denatured at 70°C (10 minutes). The NuPAGE 10% BisTris SDS Mini Polyacrylamide gel (Invitrogen) was run with 1x NuPAGE MOPS SDS Running Buffer (Invitrogen) with 200 V (1 hour and 15 minutes). MagicMark XP Western Protein Standard (Novex) and Kaleidoscope™ prestained standards (Bio-Rad) were used as standard size markers.

Table 2.3. The amount of protein loaded onto the gel for detection by Western blot.

Cell line	Protein loaded (µg)		
	CCK2 receptor	NR4A2	EGFP-NR4A2
MKN45	60	85	50
KATO-III	60	60	
AGS-G_R	60		
HEK293	60		30

The PVDF Immobilon-P membrane (pore size 0.45 µm) (Millipore Immobilon®) was activated with methanol (30 seconds) and washed in dH_2O and kept at 4°C in 1x NuPAGE Transfer Buffer supplemented with 10% methanol and 0.1% NuPAGE antioxidant (Invitrogen) until used. The proteins were transferred on to the PVDF-membrane by using Xcell II Blot Module (Invitrogen) with the use of Transfer Buffer and run with 30 V (1 hour and 10 minutes).

To visualize the success of the transfer of proteins on the PVDF membrane, a reversible membrane staining (30 seconds) was performed with Ponceau S Staining Solution (0.1% Ponceau S (Sigma- Aldrich) in 5% acetic acid). The membrane was subsequently washed in TBST (1M Trizma base (Sigma- Aldrich), 18% NaCl (Merck, Millipore), 0.1% Tween 20 (VWR)) and blocked with 5% non-fat dry milk (Nestle) in TBST (2 hours or longer if problems with unspecific bands). After blocking, the membrane was washed in TBST (3x 10 minutes). The membrane was incubated with the primary antibody (table 2.4), diluted in 5% non-fat dry milk in TBST or 1% BSA in TBST (2 hours in room temperature or at 4°C over night). Before adding secondary antibody, the membrane was washed with TBST (3x 10 minutes). The horse-radish peroxidase-conjugated secondary antibody was diluted in 5% non-fat dry milk in TBST and the membrane was incubated at room temperature (1 hour and 30 minutes).

Table 2.4. Antibodies used in Western blotting.

Antibody	Molecular weight (kDa)	Company	Dilution	Diluent
Primary				
GFP	27	Abcam	1:2000	1% BSA
NR4A2	66	Abcam	1:1000	5% non-fat dry milk
CREB	43	Cell Signaling	1:1000	5% non-fat dry milk
TCF4	58,79	Cell Signaling	1:1000	5% non-fat dry milk
TORC2	79-85	Calbiochem	1:2000	5% non-fat dry milk
CCKBR	48	Abcam	1:1000	5% non-fat dry milk
β-catenin	92	Cell Signaling	1:1000	5% non-fat dry milk
α-tubulin	55	Santa Cruz	1:1000	5% non-fat dry milk
GAPDH	36	Abcam	1:5000	5% non-fat dry milk
LKB1	54	Cell Signaling	1:1000	5% non-fat dry milk
Secondary				
Goat anti-mouse		Dako Denmark AS	1:5000	5% non-fat dry milk
Hoarse anti-rabbit		Thermo Science	1:5000	5% non-fat dry milk

The membrane was further washed in TBST (3x 10 minutes). To detect the proteins on the membrane SuperSignal® West Femto Substrate Maximum Sensitivity Substrate (Thermo Scientific) system was used. The incubation time with the substrate varied depending on the protein (40 seconds to 5 minutes) and the blots were imaged by Kodak Image Station 2000R (Kodak) or with Odyssey FC (LI-COR). To quantify the proteins, Kodak Molecular Imaging software or Image Studio was used. The relative expression levels of the proteins were detected by normalizing to α-tubulin or GAPDH and graphs were made in Prism 6 (GraphPad).

2.6 Immunoprecipitation (IP)

Immunoprecipitation is a method for precipitating proteins using an antibody that specifically binds the protein of interest (figure 2.1). It is possible to precipitate intact protein complexes, also known as co-IP. IP is a technique used for detection of protein-protein interactions [52].

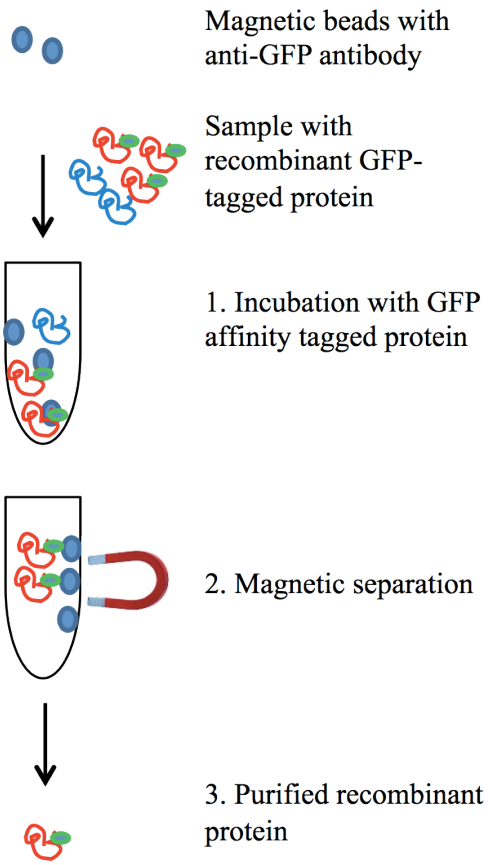

Figure 2.1. Immunoprecipitation (IP). Magnetic beads coupled to specific antibodies are incubated with the sample containing the protein of interest. Following an incubation period, the protein will bind to the bead-antibody complex. By use of a magnetic rack, the bead-antibody-protein complex immobilises to one side of the tube and allow for removal of the supernatant. The antigen can then be separated from the beads by heating.

2.6.1 Coupling of anti-GFP to Dynabeads

200 µl protein Dynabeads Protein A (Invitrogen) was washed 3x in 1 ml 0.1 M Na-phosphate buffer (pH 7.5) (Riedel de Haên) using a magnetic rack. The antibody solution was prepared by adding 10 µg anti-GFP (affinity-purified rabbit polyclonal antibody raised against GFP protein) per 100 µl diluted in Na-phosphate buffer. The beads were incubated in room temperature with antibody on a roller (1 hour). The

beads were then washed 3x in 1 ml Na-phosphate buffer, 2x in 1 ml 0.2 M Trietanolamine (pH 8.2) (Sigma) and incubated with Dimethyl pimelimidate dihydrochloride (DMP)-solution (10 mg DMP (Sigma) per 100 µl beads, dissolved in 1 ml Trietanolamine) (45 minutes). The beads were washed in 1 ml 0.1 M Etanolamine (pH 8.2) (Sigma) and then incubated with 1 ml Etanolamine (1 hour). Finally, the beads were then washed 3x in 1 ml PBS, and resuspended in 200 µl PBS with 0.1% Tween and stored at 4 °C.

2.6.2 Immunoprecipitation

HEK293 and MKN45 cells were seeded in 100mm^2 petri dishes according to table 2.1. The HEK293 cells were incubated for 48 hours, and transfected according to table 2.2, and serum starved for 24 hours. The MKN45 cells were incubated for 24 hours, and transfected according to table 2.2. The cells were starved for 48 hours prior to treatment with 10 nM gastrin (2 and 4 hours).

The cells were lysed in IP lysis-buffer (10 mM Tris (Sigma), 200 mM KCl (Sigma), 2 mM EDTA (Gibco), 40% Glycerol (Merk, Millipore), 0,5% NP40, 2 mM DTT, 10 mM $MgCl_2$ (Fluka), dH_2O, protease inhibitor cocktails 1x Complete (PI), 5x PIC2, 5x PIC3). The lysates were made following the same procedure as Western blot and the IP lysis-buffer was added 2x the volume of the cell pellet. The tubes were placed on the roller for 2 hours and vortexed (30 seconds) every 20-30 minutes. The cells were centrifuged at 4°C (16000x g, 16 minutes) and stored at -80 °C.

200 µg of protein was solved in 10 mM Tris (pH 7.5), to a total volume of 100 µl. 15 µl Dynabeads Protein A precoated with anti-GFP was washed in 1 ml Tris, and resuspended in 100 µl Tris. The beads and the proteins lysate were mixed and incubated at 4°C on a roller (over night). The beads were washed 3x in 500 µl Tris and 20 µl of loading buffer (10x DTT, 4x LDS, dH_2O) was added and incubated at 70°C (10 minutes). The beads were then removed and the samples were analysed with Western blot. For the MKN45 cells 40 µg of the cell lysate was included as input for the MKN45 cells, and 30 µg was used for the HEK293 cells. Lysate from AGS-G_R cells transfected with pEGFP-NR4A2 (10 µg) was used as a positive control for the NR4A2 antibody.

2.7 Mass Spectrometry analysis of proteins

In the first biological experiment, 200 µg of protein was used for immunoprecipitation by guidance from the Proteomics and Metabolomics Core Facility (PROMEC), NTNU. However, the results indicated that more proteins were needed to investigate protein-protein interactions. After normalisation of the MS raw-data, only a few proteins were detected and therefore the experiment had to be repeated.

In the second biological experiment, the HEK293 and MKN45 cells were seeded and transfected as described for IP. The cells were starved for 24 hours prior to stimulation with 10 nM gastrin (30 minutes). 1000 µg of protein was incubated with 20 µg Dynabeads Protein A at 4°C (over night). To optimise the washing buffer 50 mM KCl was added to increase the stringency of the buffer. The samples were resuspended in loading buffer as described for IP and analysed at PROMEC. The method is briefly described as follows: The samples were run on a 10% Invitrogen Novex gel (Invitrogen), stained with Comassie Blue, and cut into three fractions. The Mass Spectrometry analysis was run on Orbitrap Elite (Thermo Scientific) with three technical replicates of each sample. The samples were analysed using Mascot and Sequest with threshold values of ≥ 5 and ≥ 1 for scores respectively and false discovery rate ≤ 0.05. Mascot uses a statistical and geometric probability-based scoring method for scoring *peptides*, while Sequest uses descriptive parameters and correlative matching of *peptide fragments* to score peptides [53].

The samples were normalised and the $\log_2$ ratio was calculated. Network and functional analyses were performed through the use of Ingenuity Pathway Analysis (IPA) (http://ingenuity.com). The criterion used was a $\log_2$ ratio ≥ 0.58. IPA uses Fisher's Exact test to calculate the p-values. P-values ≤ 0.05 were considered significant. For the networks, a p-score is presented, and is defined as:

p-score = $-\log_{10}$ (p-value).

2.8 qRT-PCR

MKN45 cells were seeded in 6 well plates according to table 2.1, serum-starved and stimulated with 10 nM gastrin (30 minutes, 1, 2, 3, and 6 hours). The cells were lysed directly in the wells by adding 350 µl RLT-lysis buffer (1 µl β-merceptoethanol (VWR) per 1ml RLT (Qiagen)) to each well. The cell lysate was collected and stored at -80 °C.

Total RNA was extracted using RNeasy Mini Kit (Qiagen) according to the protocol recommended by the manufacturer. RNA quality and quantity were evaluated with Nanodrop spectrophotometer.

cDNA synthesis was performed using Transcriptor First Strand cDNA Synthesis Kit (Roche), with 1 µg total RNA and a total volume of 20 µl of the reaction mix. As a negative control reverse transcriptase was omitted and replaced with dH2O. The cDNA was diluted 1:2 in RNase free water, and stored at -20°C.

qRT-PCR was performed using Fast Start Universal SYBR Green master (Rox), (Roche). The protocol was followed using 2 µg cDNA, 200 nM of the primers with a total volume of 20 µl of the reaction mix. The primer sequences used are shown in table 2.5.

Table 2.5. Primers used in qRT-PCR.

Primer	Sequence
NR4A2	
NR4A2 forward	5′-GTCTCAGCTGCTCGACACG-3′
NR4A2 reverse	5′- TTTTGCACTGTGTCGCTTAAA-3′
β-actin	
β-actin forward	5′- TGAGCGCGGCTACAGCTT-3′
β-actin reverse	5′- CCTTAATGTCACGCACGATTT-3′

Real-time PCR was performed in Life Technologies StepOnePlus Real-Time PCR System: 5 minutes at 95°C, 40 cycles of 30 seconds at 95°C, 30 seconds at 60°C, 30 seconds at 72°C. Melt curve analysis was also performed with 15 seconds at 95°C, 1

minute in 60°C, and then increasing temperature by 0.3°C per second up to 95°C, and finally 15 seconds at 95°C. The melt curve is shown in appendix 2.

The PCR samples were run in triplicates and the expression levels were normalized to β-actin. The average CT-value was used for further quantification, and the ΔΔCT-method [54] was used to calculate the relative expression rate of the gene of interest. Data is presented as mean ± S.D and graphs were made in Prism 6 (GraphPad).

2.9 Immunocytochemistry

MKN45 cells were seeded in Lab-Tek^{TM} Chambered Coverglass with 8 wells (NUNC, Thermo Scientific) according to table 2.1 and incubated for 24 hours. The cells were fixated in 4% paraformaldehyde (Merck), and incubated at room temperature (10 minutes). The wells were washed with PBS. Ice-cold methanol was added to permeabilize the cells and the wells were incubated on ice (10 minutes). The methanol was removed and the wells were washed in PBS, and incubated with blocking solution (3% goat serum blocking solution (Gibco) in PBS) and incubated at 4°C (over night).

The cells were incubated with primary antibody on a shaker at room temperature (1 hour) and washed in PBS (3x 10 minutes). The cells were then incubated with the secondary antibody (1 hour), and protected from light. Antibodies used are presented in table 2.6.

Table 2.6. Antibodies used in confocal microscopy.

Antibody	Molecular weight (kDa)	Company	Dilution	Diluent
Primary				
CCK2R	48 kDa	Abbiotech	1:200	1% goat serum in PBS
CCK2R	48 kDa	Abcam	1:300	1% goat serum in PBS
Secondary				
Alexa 488		Invitrogen	1:5000	1% goat serum in PBS

The wells were further washed with PBS (4x 10 minutes) and in addition nuclear stained with Draq-5 (5 μM in PBS) (AH Diagnostics) by adding 100 μl to each well

and incubated on a shaker (5 minutes). The Draq-5 solution was removed and cold 200 µl PBS was added before confocal microscopy using LSM 510 META (Zeiss).

2.10 MTT – assay

MTT is a colorimetric viability assay that measures the reduction of yellow 3-(4,5-dimethythiazol-2-yl)-2,5-diphenyl tetrazolium bromide (MTT) to a dark purple colored formazan product [55].

HEK293 and MKN45 were seeded in 96-well plates according to table 2.1, and cultivated for 24 hours. The cells were then transfected with 0.1 µg plasmid and 0.5 µl Metafectene PRO/ well. The MTT stock solution (500 mg in 100 ml PBS) (Sigma) was diluted 1:5 in media without serum and was added into each well 48 hours after transfection and incubated at 37°C (4 hours). 130 µl of the medium was removed and 100 µl of Isopropanol (Kemetyl) (acidified to 37 % with HCl) was added before incubation on a shaker (1 hour). The absorbance of formazan was measured spectrophotometrically at 570 nm.

Possible statistical significance between the transfected cells were identified using a two-tailed independent Student´s t-test in Excel. P-value ≤ 0.05 was considered significant.

3. Results

3.1 The CCK2 receptor is expressed in MKN45 and KATO-III cells

Initially, we wanted to establish a cell line model that could easily be transfected and at the same represent as a model to study gastrin mediated NR4A2 regulation. Since only a few studies have shown the expression of the CCK2 receptor in gastric cancer cell-lines [56], and seldom at the protein level, we examined the expression in MKN45 and KATO-III cells by Western blot.

The CCK2 receptor was detected in both cell lines, utilizing the CCK2 receptor antibody from Abcam (figure 3.1 upper panel). The antibody showed some non-specific bindings, but a band at approximately 48 kDa was detected and believed to be the correct band. The strongest expression of the CCK2 receptor was observed in MKN45 cells, while the expression in KATO-III cells was rather weak. This is in accordance with other studies. The KATO-III cells has been reported to express both gastrin and the CCK2 receptor mRNA, and upon gastrin stimulation, the expression of genes associated with cell growth and anti-apoptotic effect are induced [57]. The MKN45 cells have been shown to be gastrin responsive and initiate mitogenic response to gastrin [58-60]. These studies are in contrast to McWilliams *et al.* [56] who did not detect the CCK2 receptor in the MKN45 cells. As expected, no bands were observed in HEK293 cells. Western blot was also performed with the CCK2R antibody from Abbiotech, but yield poor results (data not shown).

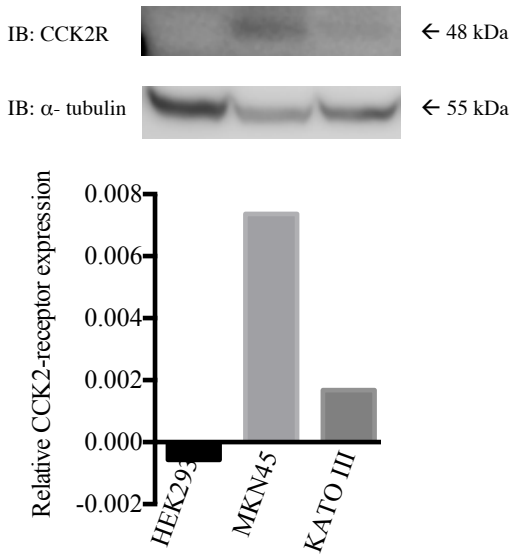

Figure 3.1. The CCK2 receptor expression in the gastric carcinoma cell lines MKN45 and KATO-III. HEK293 cells were included as a control. The data represent one of two independent experiments.

3.1.1 The expression of the CCK2 receptor determined by immunocytochemistry

Further we examined the expression of the CCK2 receptor using immunocytochemistry and confocal microscopy imaging. In this experiment two different antibodies targeting the CCK2 receptor were used (antibodies from Abbiotech and Abcam, respectively), while Alexa 488 was used as secondary antibody. The CCK2 receptor is expressed in the cytoplasm and/or plasma membrane of the MKN45 cells (figure 3.2A). The antibody from Abbiotech seems to be the most suitable for confocal imaging as the staining pattern was considerably stronger compared to almost no expression using antibodies from Abcam (figure 3.2B). Negative controls without the primary antibody showed no staining.

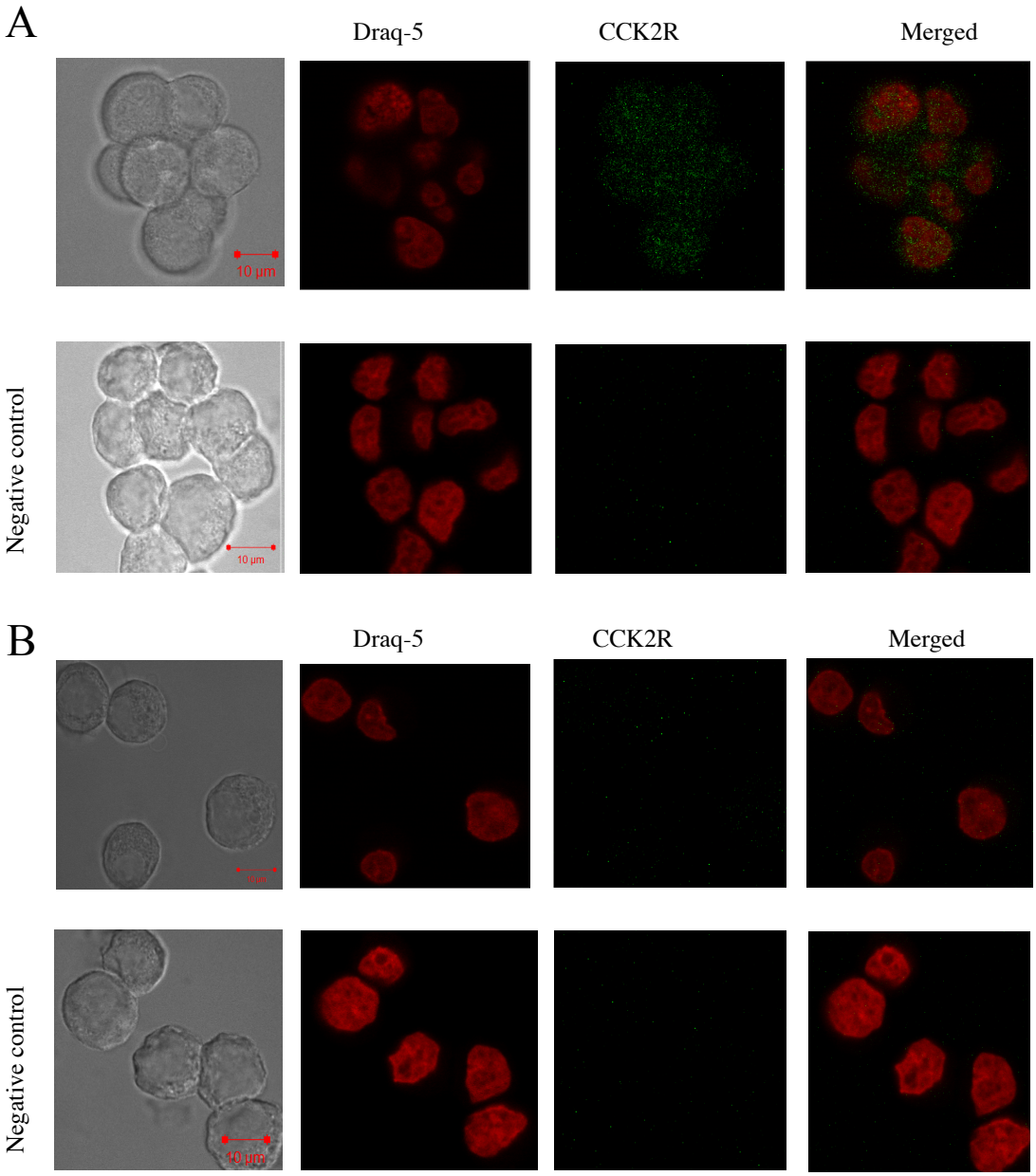

Figure 3.2. The CCK2 receptor expression in MKN45 cells. The cells were fixed and stained for the CCK2 receptor by using antibodies from Abbiotech and Abcam (A and B, respectively). The cells were co-stained with Draq-5 (red) and visualized with Alexa 488 antibodies (green) by confocal microscopy (63x magnification).

The AGS-G_R cells are stabile transfected with the CCK2-receptor [61] and confocal imaging of the CCK2 receptor with the Abbiotech show high expression of the receptor using the antibody from Abbiotech (figure 3.3.).

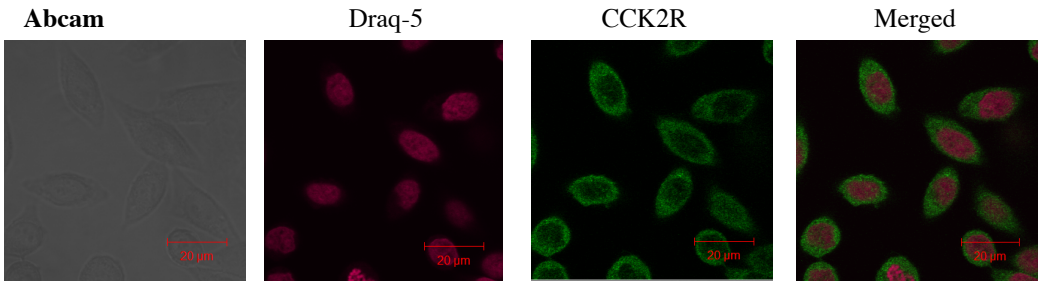

Figure 3.3. The CCK2 receptor expression in AGS-G_R cells. The cells were fixed and stained for the CCK2 receptor by using antibodies from Abbiotech. The cells were co-stained with Draq-5 (red) and visualized with Alexa 488 antibodies (green) by confocal microscopy (63x magnification). **(Experiment performed by PhD fellow Shalini Rao)**

3.1.2 Gastrin induces CCK2 receptor expression in MKN45 cells

Some studies have shown that gastrin can induce the expression of CCK2 receptor both at the mRNA [26, 62] and the protein level both *in vitro* and *in vivo* [62]. It was therefore of interest to investigate the expression of the CCK2 receptor upon gastrin stimulation in MKN45 and AGS-G_R cells.

The results indicate that gastrin induces the level of CCK2 receptor both in MKN45 and AGS-G_R cells. An increase in the protein level are observed after 8 hours of gastrin stimulation both cell lines (figure 3.4). The results are in agreement with the findings reported that the mRNA level increase upon gastrin stimulation in the AGS-G_R cells [26, 62], but has not been previously shown at protein level either in the AGS-G_R or in the MKN45 cells. The AGS-G_R cells were included as a positive control, but did not express a strong band as expected, although they express high levels of the receptor (figure 3.3).

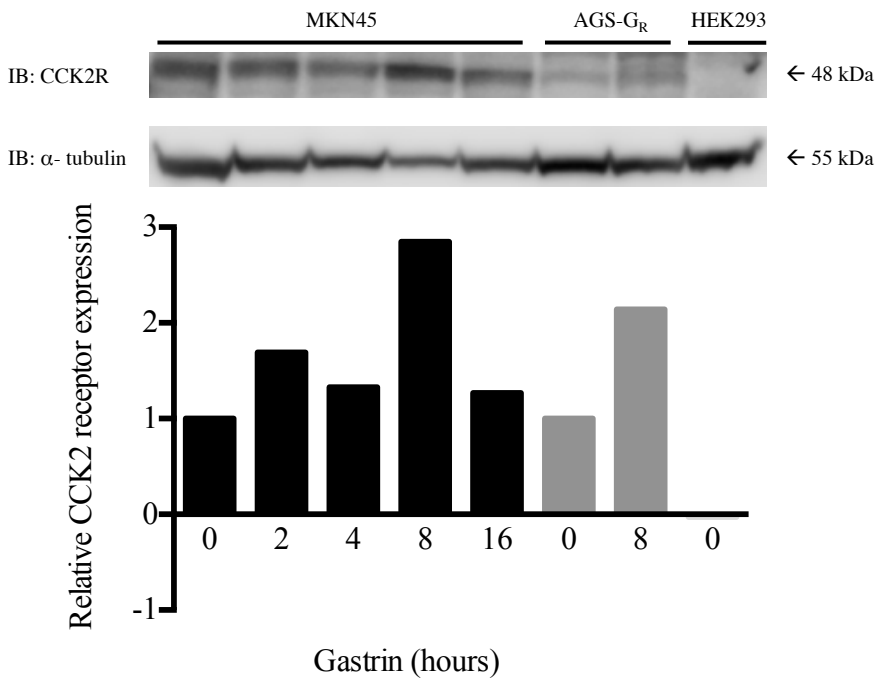

Figure 3.4. Gastrin induced CCK2 receptor expression in MKN45 and AGS-G$_R$ cells. The cells were stimulated with gastrin (10 nM) for the time points indicated. HEK293 cells were included as a control. The data represents one of two independent experiments.

3.2 The NR4A2 expression in gastric carcinomas cell lines

We have previously shown that NR4A2 is a gastrin responsive gene in the AGS-G$_R$ and AR42J cell lines [26, 51]. In the present study we investigated whether gastrin induced NR4A2 expression in MKN45 and KATO-III cells.

The mRNA expression of NR4A2 was transiently induced by gastrin with the highest expression after one hour and with a decrease to baseline after three hours (Figure 3.5A). The NR4A2 protein expression was confirmed by Western blot (figure 3.5B), and showed a peak after three hours with a subsequently decline. The expression pattern is representative of early response genes and the NR4A2 kinetic shown here is also reported by others [48, 51, 63]. Our results identify NR4A2 as a gastrin responsive gene in the adenocarcinoma cell line MKN45.

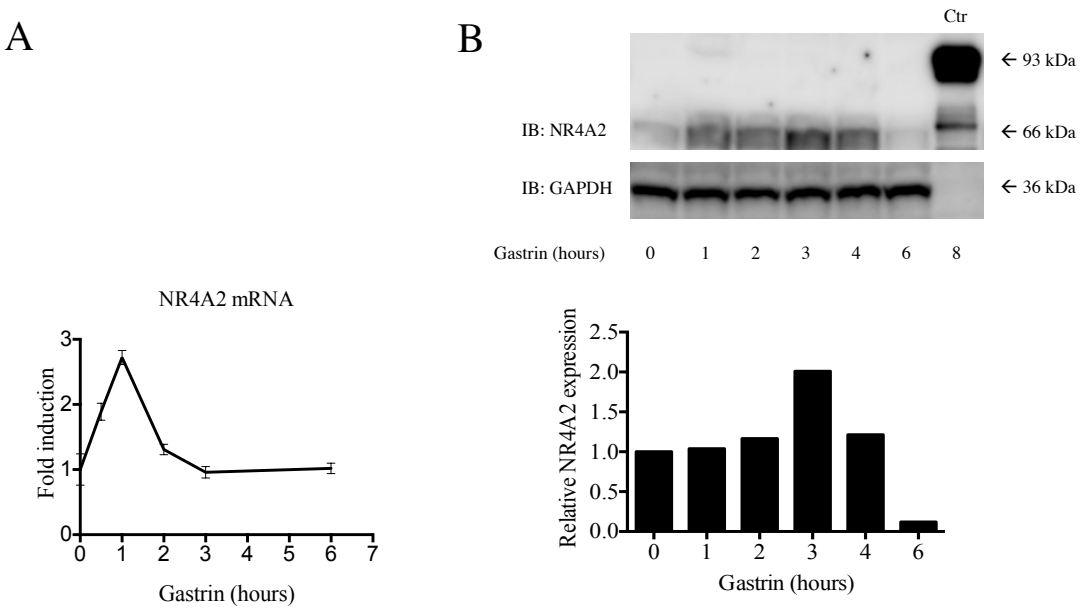

Figure 3.5. Gastrin induced NR4A2 expression in MKN45 cells. **A:** The cells were treated with gastrin (10 nM) and the mRNA levels of NR4A2 were measured with qRT-PCR. The data shown are mean ± SD. The data represent one of two biological experiments using three technical replicates. **B:** Western blot showing gastrin induced NR4A2 in MKN45 cells. AGS-G_R cells transiently transfected with pEGFP-NR4A2 were used as control. The data represent one of two independent experiments.

We next examined gastrin-induced expression of NR4A2 in KATO-III cells. The expression of NR4A2 was undetectable (figure 3.6). Therefore, no further experiments were performed in this cell line.

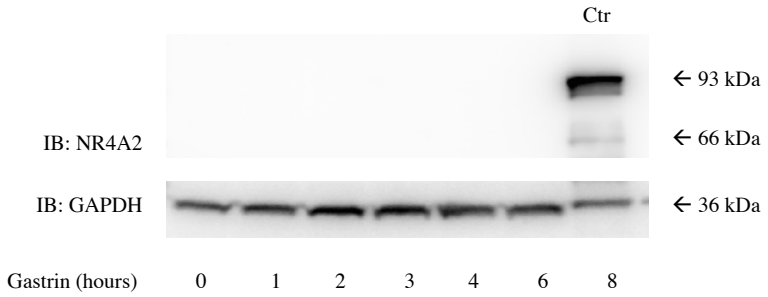

Figure 3.6. Gastrin does not induced NR4A2 expression in KATO-III cells. The cells were stimulated with gastrin (10 nM). Western blot showing no expression of NR4A2. AGS-G_R cells transiently transfected with pEGFP-NR4A2 were used as control.

3.3 Overexpression of NR4A2 in MKN45 cells and HEK293 cells

Since previous results showed low levels of NR4A2 in untreated MKN45 cells, and we wanted to perform IP to identify protein-protein interaction partners of NR4A2 we transiently transfected the cells with the expression plasmid with recombinant EGFP tagged NR4A2, pEGFP-NR4A2. The HEK293 cells were included as a non-gastric-cancer cell line as it was of interest to find novel interaction partners of NR4A2 regardless of cell line.

The transfection efficiency was determined by fluorescence microscopy, and in the MKN45 cells the number of transfected cells was estimated to be approximately 50-60% (figure 3.7A). Further, the transfection protocol for the HEK293 cell was optimised by using different amounts of plasmid and Metafectene PRO (see table 2.2 in "material and method" for details). The transfection condition "B" corresponding to 2.5 µg DNA and 6 µl Metafectene PRO, resulted in 80-90% transfection efficiency (figure 3.7B). When transfecting cells in 100 mm petri dishes, 13 µg DNA and 40 µl Metafectene PRO were used and resulted in 90% transfection efficiency. Overexpression of the EGFP-NR4A2 protein (93 kDa) was detected in both the cell lines determined by Western blotting (figure 3.8 A and B).

As NR4A2 overexpression has shown to increase apoptosis in the AGS-G_R cells [51], we wanted to examine the cell viability of the transfected cells, using MTT assay. No significant differences (p-value ≤ 0.05) in cell viability were detected in MKN45 or HEK293 cells, appendix 3.

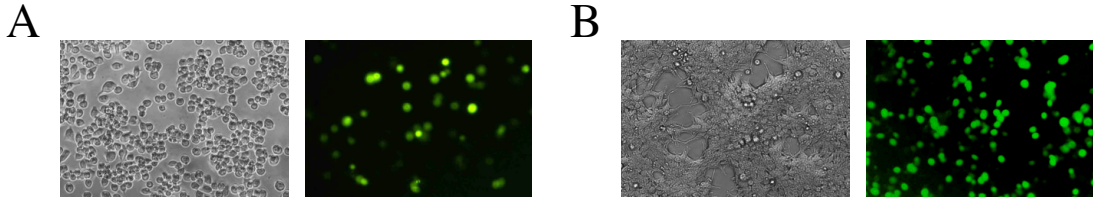

Figure 3.7. Overexpression of NR4A2 in transiently transfected cells. MKN45 cells and HEK293 cells (A and B, respectively) were transfected with pEGFP-NR4A2 and visualised by inverted fluorescence microscopy (400x magnification) before and after use of the EGFP filter, left and right panel respectively.

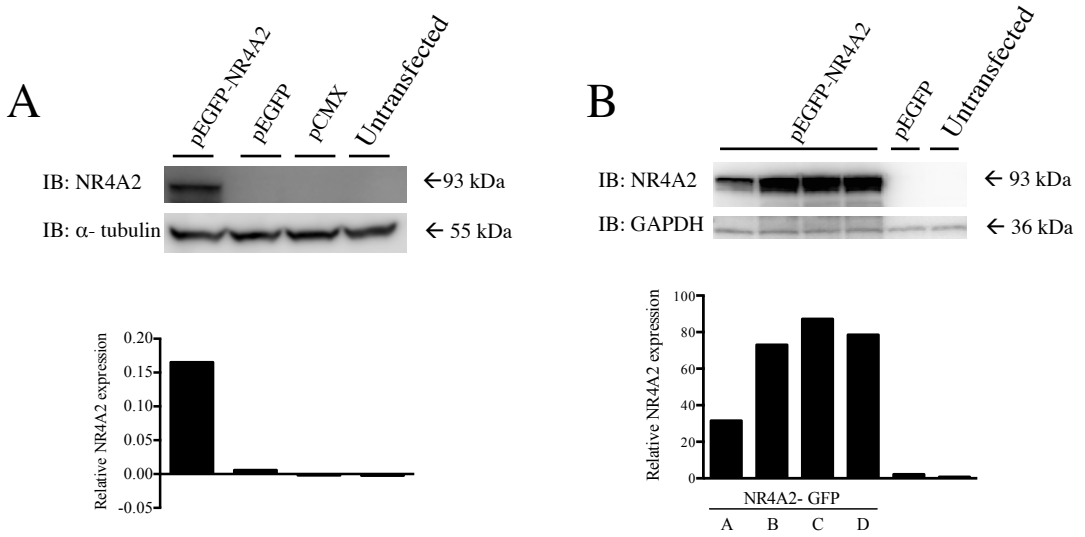

Figure 3.8. Expression of EGFP-NR4A2. A: MKN45 cells were transfected with pEGFP-NR4A2, pEGFP or pCMX and the expression of EGFP-NR4A2 was validated by Western blot. **B:** HEK293 cells were transfected with pEGFP and pEGFP-NR4A2 with different ratios of the plasmid and metafectene PRO (A, B, C, D) as described in table 2.2 in "Material and method". The expression of EGFP-NR4A2 was determined by Western blot.

3.4 NR4A2 does not bind to CREB or β-catenin

To elucidate the role of NR4A2 in MKN45 cells it was of interest to characterize interaction partners of NR4A2. Initially immunoprecipitation was performed with antibodies targeting proteins known from the literature to be crucial in gastric adenocarcinoma cells. The Wnt/β-catenin signalling pathway is often deregulated in gastric cancer [64, 65]. Some nuclear receptors, e.g. the androgen receptor (AR) are known to modulate the Wnt-signalling pathway by interactions with β-catenin directly, whereas others have shown to bind to other members of the signalling pathway including Wnt, T cell factors (TCF) or glycogen synthase kinase-3 β (GSK3β) [66]. We therefore investigated whether a direct interaction could be found between NR4A2 and β-catenin or TCF4. Moreover, cAMP response element-binging protein (CREB) is a transcription factor shown by our group and others to play a role in gastrin-mediated signalling [67, 68] and is involved in cellular responses like growth and survival [69]. It was therefore of interest to examine a putative NR4A2-CREB interaction.

NR4A2 protein was detected in the cells overexpressing pEGFP-NR4A2, confirming the transfection (figure 3.9). In the MKN45 cells no bands were detected using

antibodies targeting β-catenin or CREB, suggesting that CREB and β-catenin do not directly interact with NR4A2. We anticipated that the binding partners might change after gastrin stimulation, expecting post-translational modifications to occur and new interactions to be formed, however, no detection of β-catenin was found in either untreated or cells treated with gastrin. Notably, TCF4 was detected in both the control and the cells expressing pEGFP-NR4A2, indicating that the TCF4 most likely interacts with the GFP-tag or the magnetic beads.

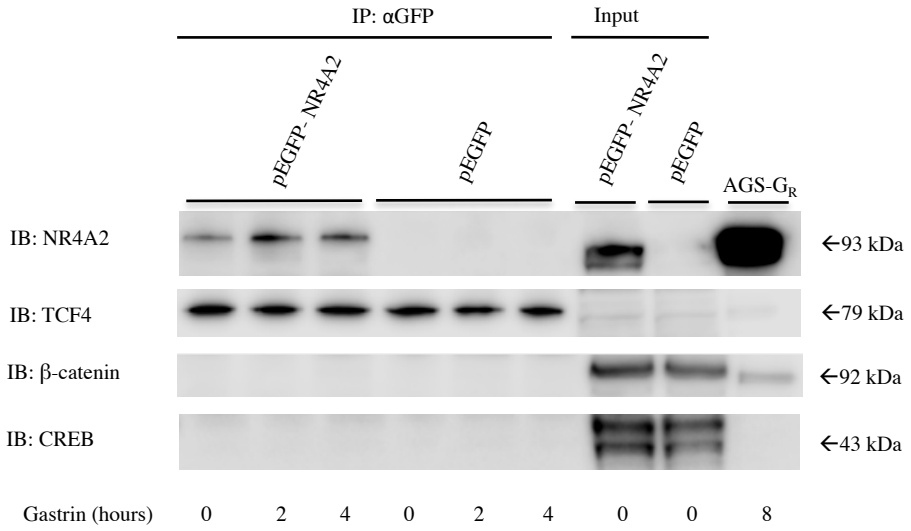

Figure 3.9. NR4A2 does not interact with TCF4, β-catenin or CREB in MKN45 cells. The cells were transfected with pEGFP-NR4A2 or pEGFP and treated with gastrin (10 nM). Cell extracts were immunoprecipitated and immunoblotted with the indicated antibodies. Total extracts (input) and AGS-G_R cells transiently transfected with pEGFP-NR4A2 was used as control. The data represents one of two independent experiments.

The HEK293 cell line is frequently used when working with recombinant proteins [70]. Kitagawa *et al.* [71] reported NR4A2 to bind to β-catenin. In the HEK293 cells no bands were detected using β-catenin and CREB antibodies (figure 3.10), which indicates that neither β-catenin nor CREB interacts with NR4A2 in these cells. This is in accordance with the findings of Rajalin & Aarnisalo that did not detect a direct interaction with β-catenin and NR4A2 in the U2-OS cells [72]. Notably, it is important to note that the paper from Kitawaga *et al.* was retracted from Molecular and Cellular Biology [71].

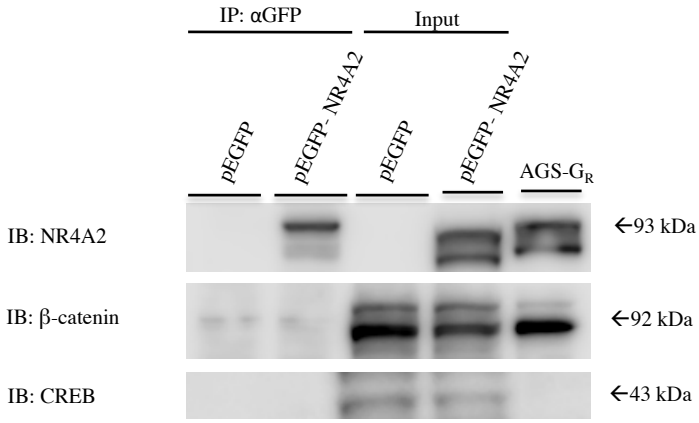

Figure 3.10. NR4A2 does not interact with β-catenin or CREB in HEK293 cells. The cells were transfected with pEGFP-NR4A2 or pEGFP. Cell extracts were immunoprecipitated and immunoblotted with the indicated antibodies. Total extract (input) and AGS-G_R transiently transfected with pEGFP-NR4A2 cell lysate was used as control. The data represent one of two independent experiments.

3.5 NR4A2 binding proteins detected by Mass Spectrometry

To get an overview of all the protein-protein interactions with NR4A2 in both the cell lines, we decided to use a Mass Spectrometry-based approach on the IP samples. Initially, to verify the transfection of the samples, 200 µg of the IP samples were immunoblotted for anti-GFP and anti-NR4A2 (figure 3.11).

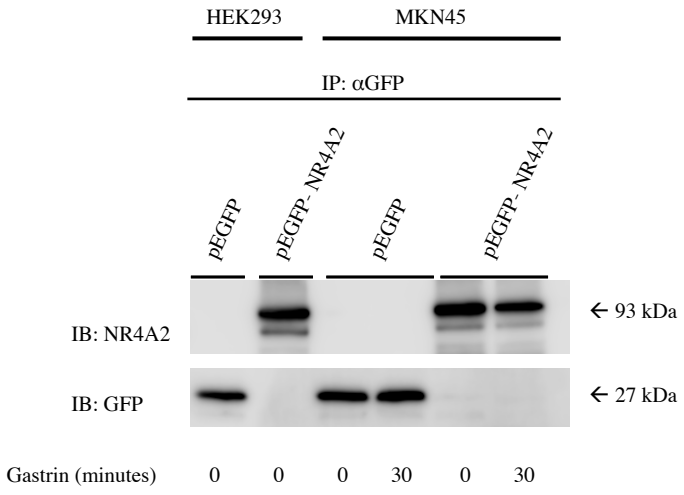

Figure 3.11. Expression of EGFP-NR4A2 or EGFP. The cells were transfected with pEGFP-NR4A2 and pEGFP. Cell extracts were immunoprecipitated and immunoblotted with the indicated antibodies.

The MS results were analysed with the two algorithms, Sequest and Mascot, which scores peptides and peptide fragments, respectively. The total number of proteins

detected by MS in both the cell lines was 453. The samples were normalised and the $\log_2$ ratio of the samples were calculated. By using this approach we detected many new potential binding partners of NR4A2. The detection cut-off in IPA was decided to be $\log_2$ ratio ≥ 0.58, meaning that the proteins that bind to both EGFP-NR4A2 and EGFP are still included in the analysis if they bind 1.5 more to EGFP-NR4A2 compared to EGFP. The complete lists of potential interacting partners of NR4A2 in both MKN45 and HEK293 are shown in Appendix 4. The results are summarized in the Venn diagram (figure 3.12).

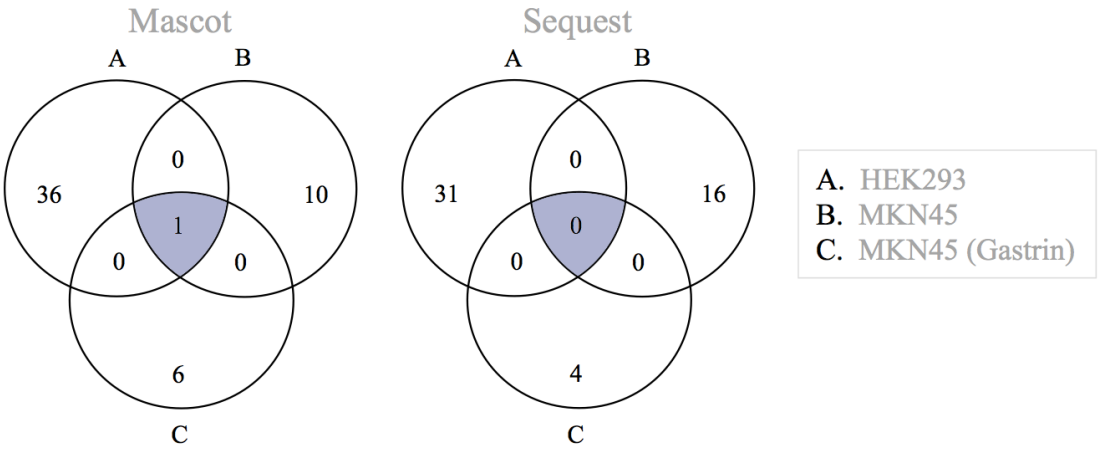

Figure 3.12. Venn diagram of the proteins detected by Mascot and Sequest.

Ingenuity Pathway Analysis (IPA) was used as a tool for annotations and visualization of the data. The proteins identified had a range of different biological functions including regulators of transcription, phosphatases, kinases and enzymes. Networks and functional analyses were generated for each sample to determine if the proteins in the dataset were interacting with each other and whether there were overlap between the datasets and well-known molecular functions and diseases. The highest scoring network for each of the samples is presented, whereas the remaining networks are presented in appendix 5. The 3 most interesting of the top 5 molecular functions and diseases are represented in the tables.

3.5.1 IPA analyses of the proteins detected in MKN45 cells

The whole dataset was uploaded on to Ingenuity Pathway Analysis to generate protein-protein interaction network. Of the proteins detected using the Sequest algorithm, 16 proteins scored a $\log_2$ ratio ≥ 0.58. Of this 3 statistically significant

networks were generated. The highest scoring network had a score of 26, meaning that there is a 1 in 10^{26} chance of this network to occur by random chance. The networks consisted of 35 proteins, whereas 10 of the proteins were found in the dataset. The network was annotated to functions like i) cellular development, ii) connective tissue development and function and iii) cellular assembly and organization (figure 3.13). A functional analysis in IPA was further performed to uncover proteins in the dataset that overlap with well-established molecular functions and diseases, presented in table 3.1. As expected the analysis showed interactions with proteins regulated in tumorigenesis and gastrointestinal disease.

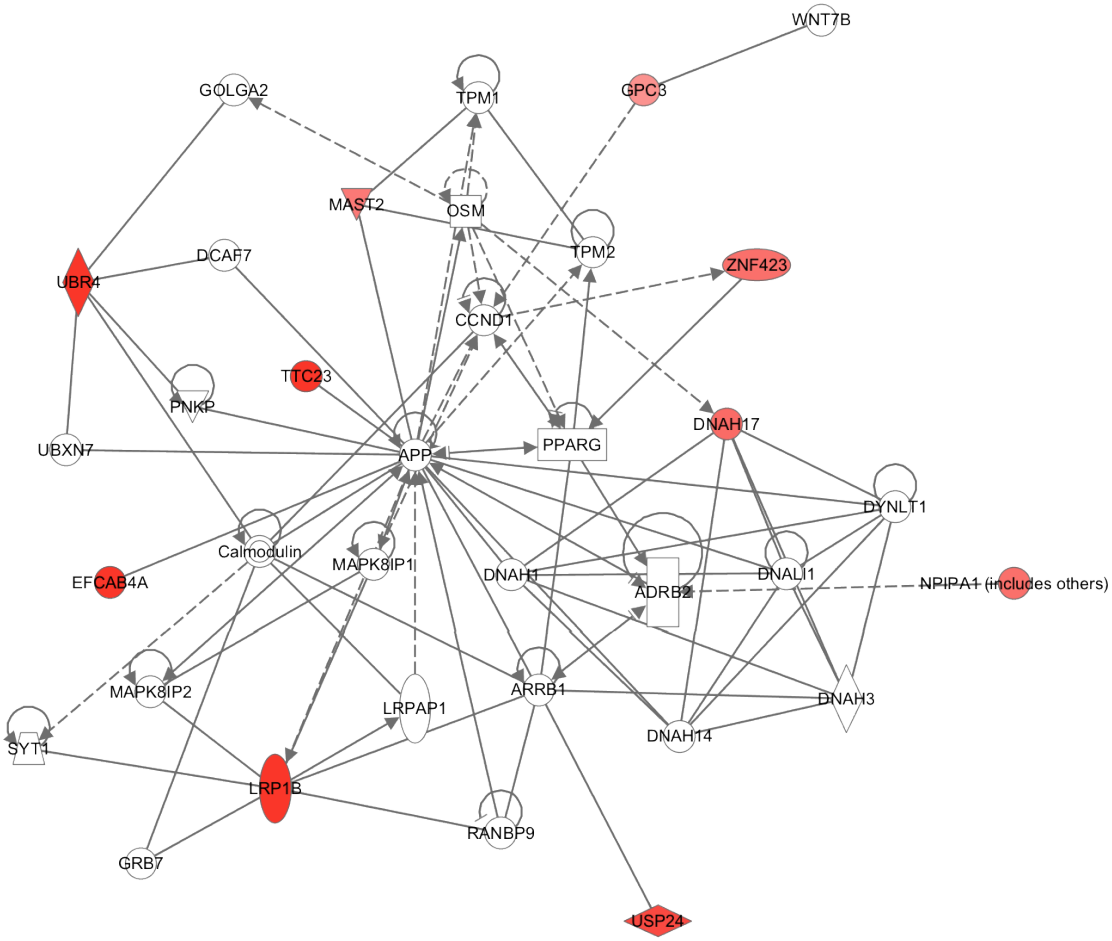

Figure 3.13. Network of proteins detected by the Sequest algorithm in MKN45 cells. The network consists of 35 molecules and is annotated to cellular development, connective tissue development and function and cellular assembly and organization. Red color indicates positive values, gray color represents proteins that did not meet the cut-off value, and white is proteins from IPA knowledge database associated with proteins in the network. Solid and dashed lines indicate direct and indirect interactions between proteins, respectively.

Table 3.1. IPA analysis of proteins found by the Sequest algorithm in MKN45 cells. Biological functions and diseases associated with the proteins found to bind to NR4A2.

	Proteins	P-value
Molecular and cellular functions		
Cellular function and maintenance	GPC3, LRP1B, UBR4, ZNF423, LGR4	6.78E-04-3.21E-02
Cellular development	GPC3, LGR4, ZNF423, MAST2, TDRD6, HDAC9	1.36E-03-4.65E-02
Cell growth and proliferation	GPC3, LGR4, ZNF423	1.36E-03-3.83E-02
Disease and disorders		
Cancer	DNAH17, LGR4, RPL4, ZNF423, GEMIN4, LRP1B, TDRD6, GPC3, MAST2, UBR4, HDAC9, PVRIG, USP24	3.82E-05-4.26E-02
Gastrointestinal Disease	DNAH17, LRP1B, UBR4, GEMIN4, MAST2, USP24, GPC3, RPL4, LGR4, TDRD6	6.78E-04-3.27E-02
Neurological disease	HDAC9, ZNF423	6.78E-04-4.84E-02

When analysing the proteomic data by the Mascot algorithm, 11 proteins above the threshold were detected. Mascot and Sequest detected no common proteins with $\log_2$ ratio ≥ 0.58. According to PROMEC, typically 60-80% overlap in the results from Mascot and Sequest are found when analysing cell extract, however, MS performed on IP extracts gives more variations in the identification of proteins. The protein network made of the proteins detected by Mascot contained 10 of the 11 proteins, and was annotated to i) tissue morphology, ii) cell morphology, and iii) cellular assembly and organization (score of 30) (figure 3.14). Notably, both the algorithms annotated many of the same molecular functions and diseases (table 3.2), indicating that both the algorithms should be valuated to the same degree.

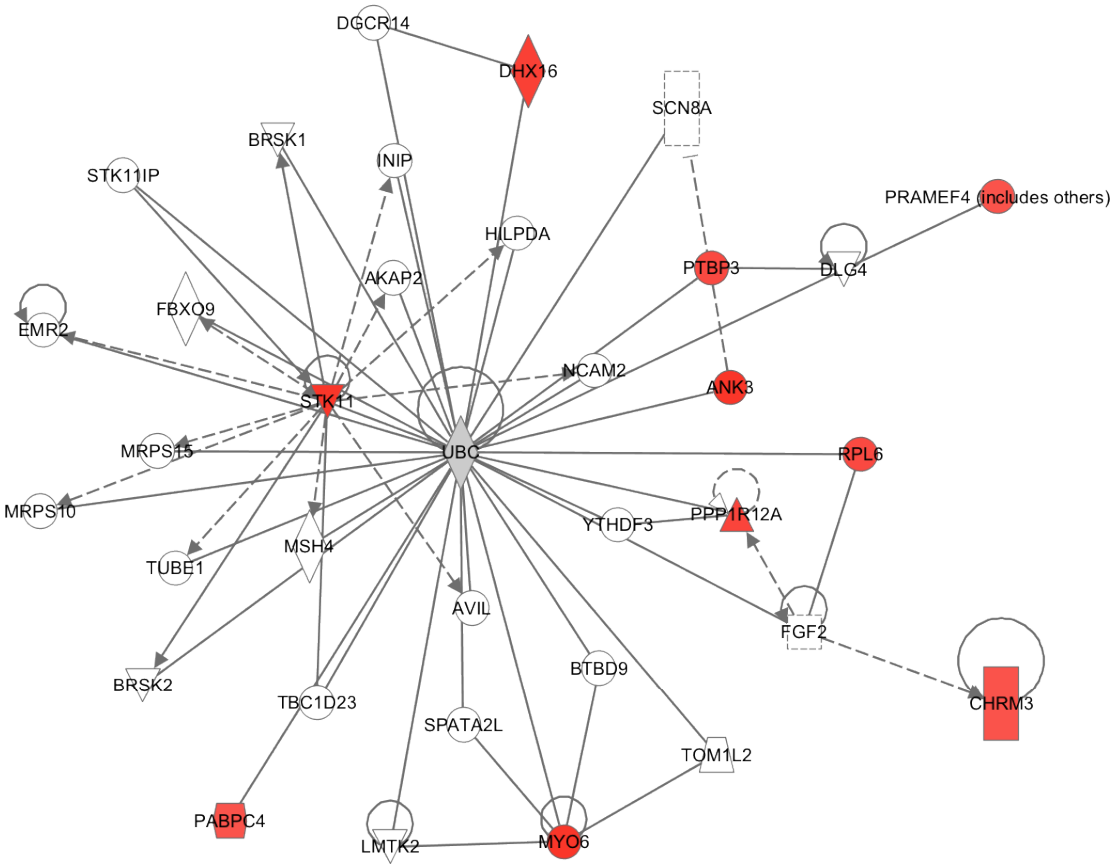

Figure 3.14. Network of proteins detected by the Mascot algorithm in MKN45 cells. The network consists of 35 molecules and is annotated to tissue morphology, cell morphology, and cellular assembly and organization. Red color indicates positive values, gray color represents proteins that did not meet the cut-off value, and white is proteins from IPA knowledge base associated with proteins in the network. Solid and dashed lines indicate direct and indirect interactions between proteins, respectively.

Table 3.2. IPA analysis of proteins found by the Mascot algorithm in MKN45. Biological functions and diseases overlapping with the proteins found to bind to NR4A2.

	Proteins	P-value
Molecular and cellular functions		
Cellular function and maintenance	ANK3, MYO6, PPP1R12A, STK11, CHRM3	4.38E-04-3.28E-02
Cell cycle	STK11, CHMR3, PPP1R12A	5.74E-04-3.22E-02
Cellular assembly and organization	ANK3, MYO6, PPP1R12A, STK11, CHMR3	5.74E-04-3.26E-02
Disease and disorders		
Cancer	ANK3, CHMR3, STK11, MYO6, PPP1R12A, DHX16, TRIM58, RPL6	5.74E-03-1.37E-02
Developmental disorders	ANK3, CHRM3, STK11, MYO6	5.74E-03-2.39E-02
Gastrointestinal Disease	ANK3, CHRM3, STK11, MYO6, PPP1R12A, DHX16, TRIM58	5.74E-03-4.39E-02

3.5.2 IPA analyses of the proteins detected in gastrin treated MKN45 cells

We have recently shown that gastrin influences the NR4A2 nucleus/cytosol shuttling in AGS-G_R cells [51]. We hypothesized that gastrin may induce similar effects in MKN45, and the cells were therefore treated with gastrin (30 minutes) before the MS analysis. Stimulated MKN45 cells overexpressing EGFP-NR4A2 were compared to stimulated controls overexpressing EGFP. The network analysis of the 4 proteins detected by the Sequest algorithm were annotated to functions associated with i) cellular function and maintenance, ii) molecular transport, and iii) cellular assembly and organization (score of 12) (figure 3.15). The functional analysis is shown in table 3.3.

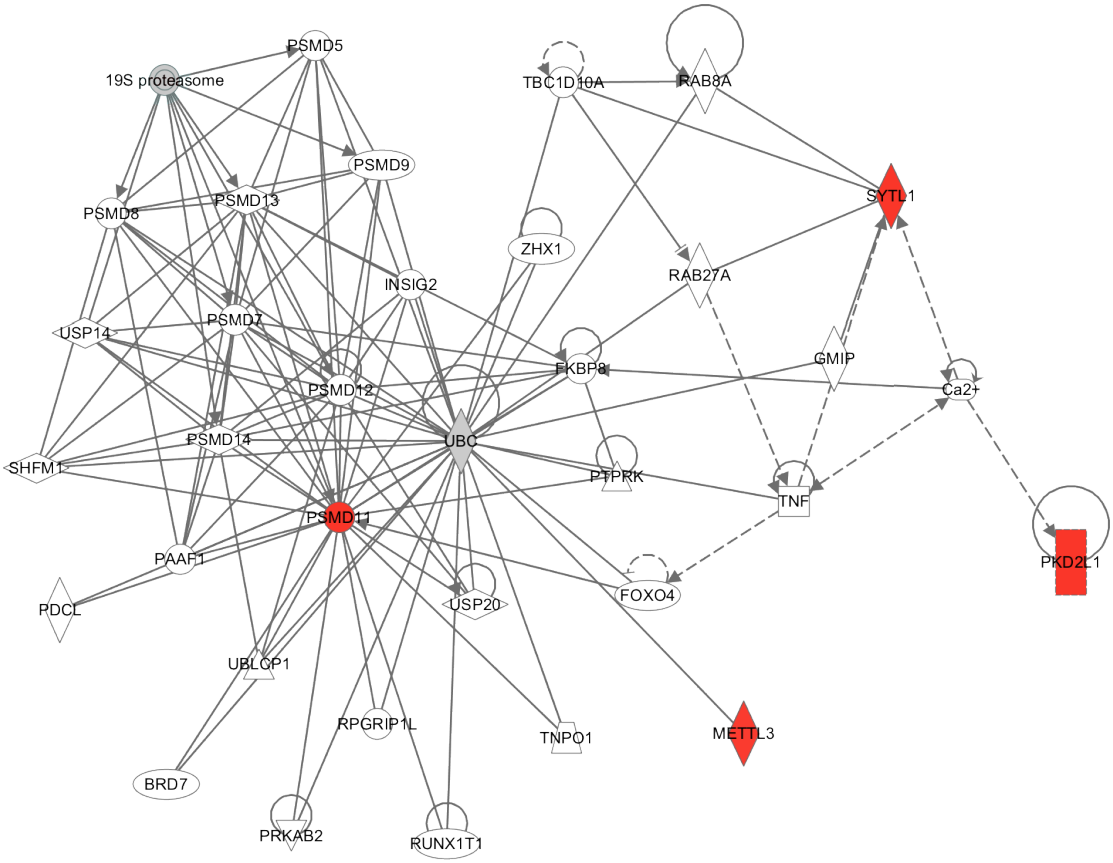

Figure 3.15. Network of proteins detected by the Sequest algorithm in MKN45 cells treated with gastrin. The network consists of 35 molecules and is annotated to cellular function and maintenance, molecular transport, and cellular assembly and organization. Red color indicates positive values, gray color represents proteins that did not meet the cut-off value, and white is proteins from IPA knowledge base associated with proteins in the network. Solid and dashed lines indicate direct and indirect interactions between proteins, respectively.

Table 3.3. IPA analysis of proteins found by the Sequest algorithm in MKN45 cells treated with gastrin. Biological functions and diseases overlapping with the proteins found to bind to NR4A2.

	Proteins	P-value
Molecular and cellular functions		
Cellular assembly and organization	SYTL1	2.09E-04-1.67E-03
Cellular function and maintenance	SYTL1	2.09E-04-2.22E-02
Molecular transport	SYTL1, PKD2L1	2.09E-04-2.34E-03
Disease and disorders		
Endocrine System disorders	SYTL1	1.67E-03-1.67E-03
Gastrointestinal disorders	SYTL1	1.67E-03-1.67E-03

The Mascot algorithm detected 7 proteins. These proteins were all found in the network associated with i) hereditary disorder, ii) neurological disease and iii) psychological disorders (score of 21) (figure 3.16). The molecular functions and diseases associated with the proteins detected are listed in table 3.4. After treatment with gastrin, different protein interaction was detected. However, one protein was detected by Mascot in both cell lines, 60S ribosomal protein L6 (RPL6), which has been shown to be higher expressed in gastric cancer tissue compared to normal gastric mucosa [73]. In the present study, the overall number of proteins detected in the stimulated cells was lower compared to the untreated cells. This suggests that the results should be interpreted critically and the experimental setup should be repeated.

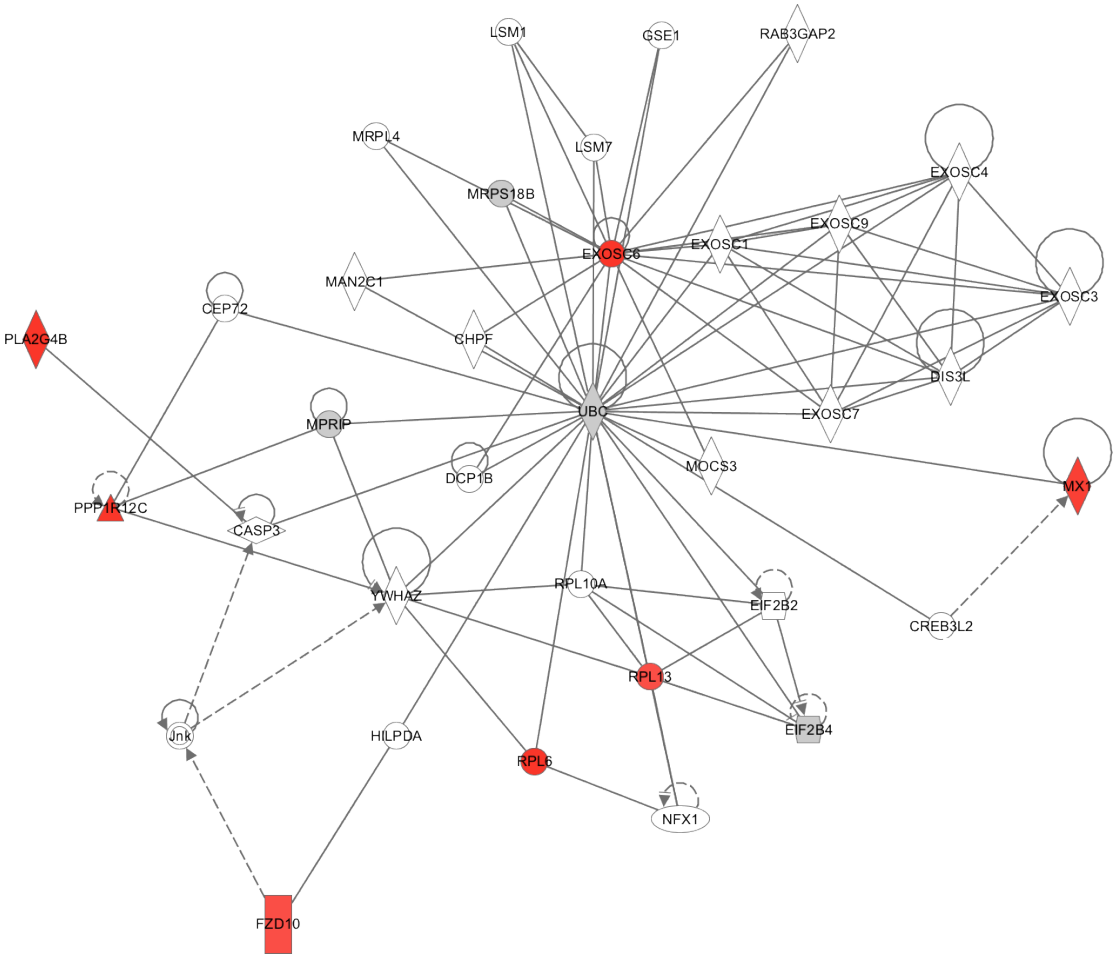

Figure 3.16. Network of proteins detected by the Mascot algorithm in MKN45 cells treated with gastrin. The network consists of 35 molecules and is annotated to hereditary disorder, neurological disease and psychological disorders. Red color indicates positive values, gray color represents proteins that did not meet the cut-off value, and white is proteins from IPA knowledge base associated with proteins in the network. Solid and dashed lines indicate direct and indirect interactions between proteins, respectively.

Table 3.4. IPA analysis of proteins found by the Mascot algorithm in MKN45 cells treated with gastrin. Biological functions and diseases overlapping with the proteins found to bind to NR4A2.

	Proteins	P-value
Molecular and cellular functions		
Lipid metabolism	MX1, PLA2G4B	3.13E-04-1.25E-03
Cell cycle	PPP1R12C	3.13E-03-3.13E-03
Cell death and survival	MX1	4.38E-03-4.38E-03
Disease and disorders		
Infectious disease	MX1	3.13E-04-3.09E-02
Cancer	MX1, RPL13, RPL6	6.53E-04-2.39E-02
Inflammatory disease	MX1	1.22E-02-4.82E-02

3.5.3. IPA analysis of the proteins detected in HEK293

Overall, more proteins were detected in HEK293 cells compared to the MKN45 cells, however the network gave very similar results for those detected in MKN45 cells. 31 proteins were detected in the HEK293 cells using the Sequest algorithm. Three statistically significant networks were generated. The highest scoring network contained 27 proteins associated with i) cellular assembly and organization, ii) cellular function and maintenance, and iii) developmental disorders (score 82) (figure 3.17). The molecular functions and diseases associated with the proteins detected by Sequest are listed in table 3.5. Proteins with similar functions as those found in MKN45 are detected in the HEK293 cells as well.

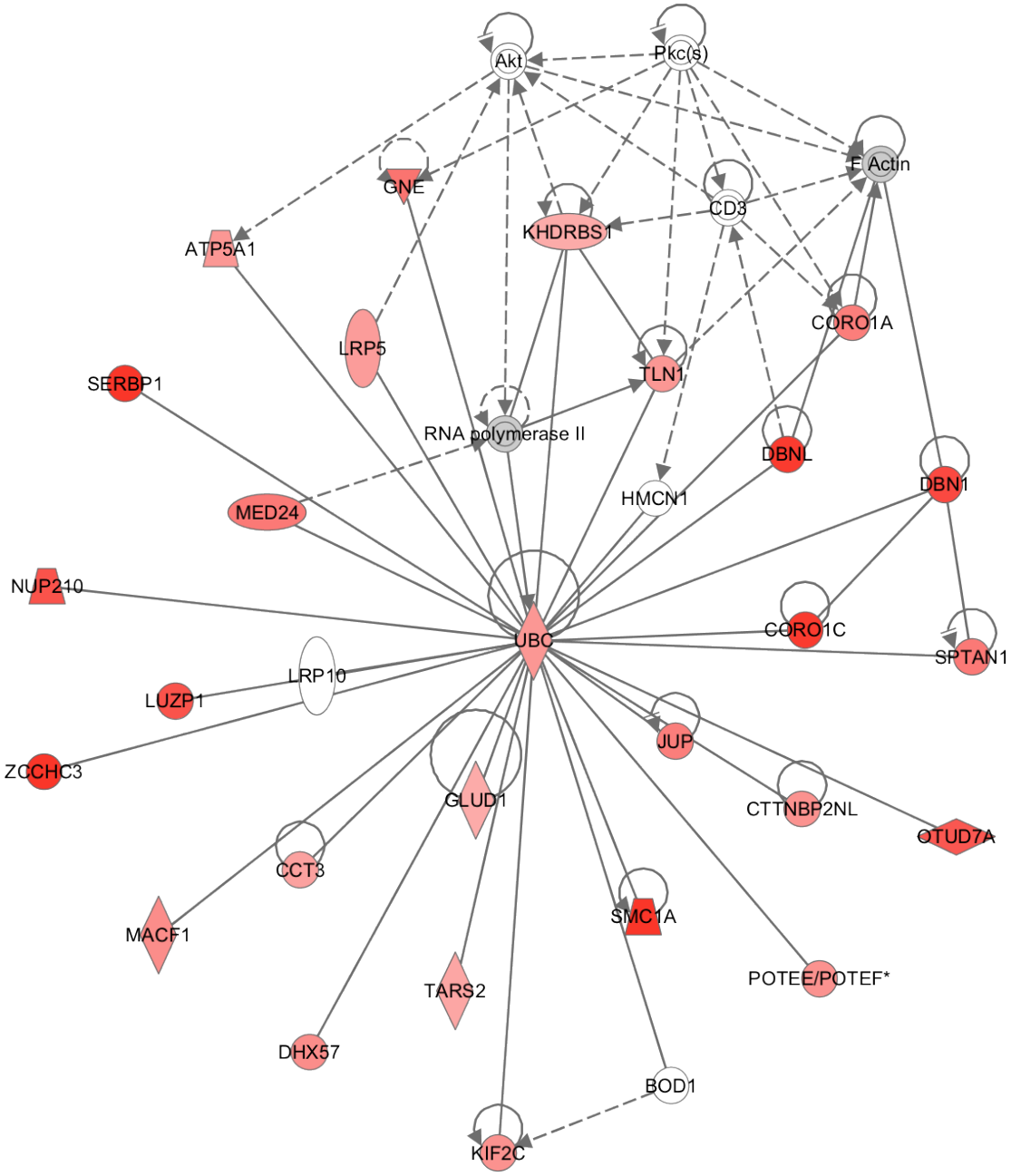

Figure 3.17. Network of proteins detected by the Sequest algorithm in HEK293 cells. The network consists of 35 molecules and is annotated to cellular assembly and organization, cellular function and maintenance, and developmental disorders. Red color indicates positive values, gray color represents proteins that did not meet the cut-off value, and white is proteins from IPA knowledge base associated with proteins in the network. Solid and dashed lines indicate direct and indirect interactions between proteins, respectively.

Table 3.5. IPA analysis of proteins found by the Sequest algorithm in HEK293 cells. Biological functions and diseases overlapping with the proteins found to bind to NR4A2.

	Proteins	P-value
Molecular and cellular functions		
Cell assembly and organization	CORO1A, CORO1C, DBN1, JUP, SPTAN1, TLN1, KIF2C, DBNL, SMC1A	7.00E-06-4.44E-02
Cellular function and maintenance	CORO1A, CORO1C, DBN1, JUP, SPTAN1, TLN1, KIF2C, SMC1A, KHDRBS1, LRP5	7.00E-06-3.81E-02
Cell-to-cell signalling and interactions	JUP, TLN1, DBN1, SERBP1, LRP5, CORO1A	1.62E-03-3.66E-02
Disease and disorders		
Cardiovascular disease	JUP, LRP5	1.62E-03-4.44E-02
Developmental disorder	JUP, LRP5, GNE, GLUD1, SMC1A	1.62E-03-1.92E-02
Gastrointestinal disease	GLUD1	1.62E-03-1.62E-03

37 proteins were detected in HEK293 cells by the Mascot algorithm and two networks were generated. The highest scoring network developed by IPA contains 23 of the proteins and was associated with i) cellular assembly and organization, ii) developmental disorder, and iii) hereditary disorder (score of 62) (figure 3.18). The molecular functions and diseases associated with the proteins detected by Mascot (table 3.6) are partly overlapping with Sequest. Both the algorithms detect three proteins in common, CORO1A, SMC1A and DBN1. CORO1A is a member of the WD-repeat actin binding proteins that have been shown to regulate cytoskeleton and membrane trafficking [74]. Mutation in SMC1A are responsible for the genetic disorder Cornelia de Lange syndrome and has been speculated to play a role in carcinogenesis [75]. DBN1 is suggested to be involve in colorectal cancer metastasis [76].

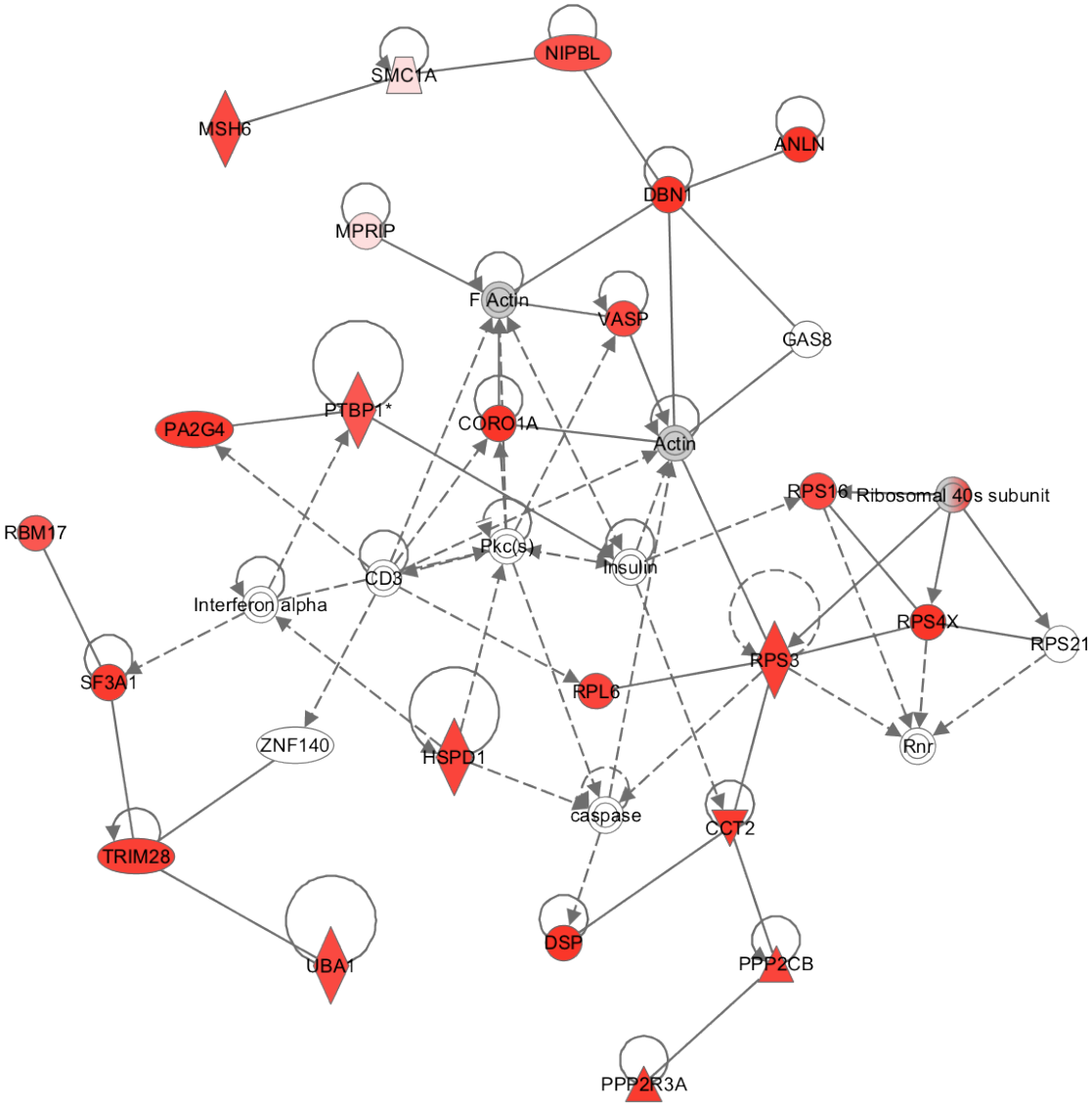

Figure 3.18. Network of proteins detected by the Mascot algorithm in HEK293 cells. The network consists of 35 molecules and is annotated to cellular assembly and organization, developmental disorder, and hereditary disorder. Red color indicates positive values, gray color represents proteins that did not meet the cut-off value, and white is proteins from IPA knowledge base associated with proteins in the network. Solid and dashed lines indicate direct and indirect interactions between proteins, respectively.

Table 3.6. IPA analysis of proteins found by the Mascot algorithm in HEK293 cells. Biological functions and diseases overlapping with the proteins found to bind to NR4A2.

	Proteins	P-value
Molecular and cellular functions		
RNA post-transcriptional modifications	DDX17, DDX54, PTBP1, RBM17, RBMX, RPS16, SF3A1	1.55E-06-2.48E-02
Cell assembly and organization	ANLN, CORO1A, DBN1, DSP, DST, LIG3, MPRIP, MSH6, NIPBL, PTBP1, SMC1A, TIMM50, VASP	2.17E-05-4.35E-02
Cell death and survival	ANLN, CCT2, CORO1A, DDX17, DSP, DST, HSPD1, LIG3, MPRIP, MSH6, PA2G4, PPP2R3A, RBM17, RPS3, SF3A1, SMC1A, TIMM50, TRIM28, UBA1, VASP	5.10E-04-4.90E-02
Disease and disorders		
Developmental disorder	DST, ALDH18A1, DSP, UBA1, VASP, SMC1A, NIPBL	3.61E-05-5.78E-03
Hereditary disorder	NIPBL, SMC1A, DSP, ALDH18A1, MSH6, DST, UBA1, HSPD1	3.61E-05-1.91E-02
Cancer	COPE, CORO2A, DBN1, DDX17, DSP, DST, EPPK1, HSPD1, LIG3, MPRIP, MSH6, MYO1D, NIPBL, PTBP1, RBMX, RPL6, RPS3, RPS16, RPS4X, SF3A1, SMC1A, UBA1, VASP	6.47E-05-4.02E-02

The content source of IPA, Ingenuity Knowledge Base, includes manually curated data from published literature, internally curated knowledge and manually reviewed content from databases and other sources (http://ingenuity.com). The networks had different amount of proteins, and a high network score is seen with a higher number of proteins. A score ≥ 1.3 (p-value ≤ 0.05) indicates a 95% confidence that the network is not generated by random. The scores of the networks represented varied from 12-82 and were considered significant.

The $\log_2$ ratios alone do not identify the proteins as interaction partners, therefor the protein interactions detected need to be further confirmed and validated through *in vitro* experiments to identify true interaction partners of NR4A2. To verify the interaction between NR4A2 and Serine/threonine-protein kinase STK11 (STK11), the IP lysate made from the MKN45 cells were analysed by Western blot with antibodies targeting STK11. The result (figure 3.19) shows that STK11 binds to both EGFP-NR4A2 and EGFP, indicating that further optimization is needed. Another approach to validate the interaction between NR4A2 and STK11 may be by confocal imaging, to determine co-localization.

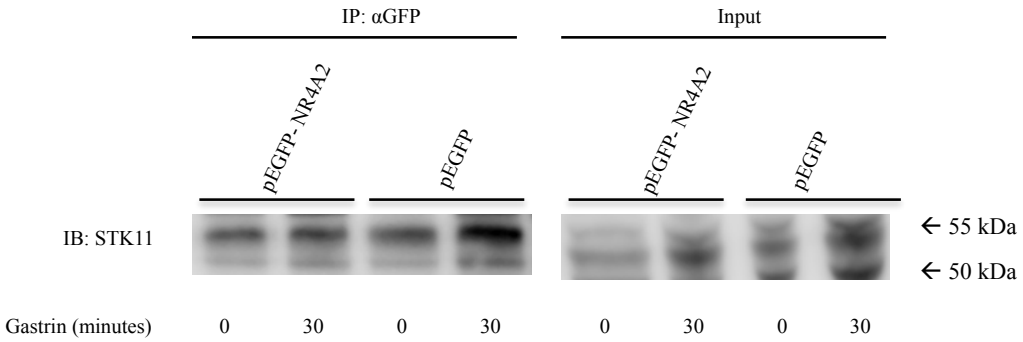

Figure 3.19. STK11 bind both EGFP-NR4A2 and EGFP in MKN45 cells. The cells were transfected with pEGFP-NR4A2 or pEGFP and treated with gastrin (10 nM). Cell extracts were immunoprecipitated and immunoblotted with the antibody targeting STK11. Total extracts (input) was used as control.

5.0 Discussion

The role of gastrin in gastric adenocarcinoma has been debated for many years, and it still remains unclear. Knowledge of gastrin-mediated molecular mechanisms and target genes can contribute to a better understanding of its role in carcinogenesis, as well as its normal function. In the present study, we have shown that gastrin induces the expression of NR4A2 in the gastric adenocarcinoma cell line MKN45. NR4A2 has been described as a putative prognostic marker in gastric cancer. To further elucidate its role, NR4A2 was overexpressed in the MKN45 and HEK293 cells. No interactions were observed between NR4A2 and the proteins initially hypothesized to bind to NR4A2. However, Mass Spectrometry (MS) in combination with Immunoprecipitation (IP) identified several potential binding partners. This thesis provides an overview of putative interactions partners of NR4A2 that may be important in gastric cancer.

The NR4A family of transcription factors have been shown to affect the cellular responses and the subcellular localization seems to be important for their function in regulation of cell survival [46, 77]. Generally, it appears that in the nucleus the NR4A receptors regulate transcription implicated in differentiation and survival [78, 79]. A cytoplasmic localization of NR4A2 has been proposed as a prognostic factor in bladder cancer and was associated with lower survival rate [30]. The proposed mechanism comprised the translocation of NR4A2 to the cytoplasm, which allows cells to invade and metastasize because of the termination of its role in transcription [30]. Pro-apoptotic roles have been shown for NR4A1 and NR4A3, which include translocation to mitochondria, interaction with Bcl-2 proteins and promotion of cell death [80, 81]. This reveals an additional mechanism other than regulation of transcription.

Generally, by use of MS in combination with IP several proteins can be identified in a single experiment, and typically 70-600 proteins are identified [82]. For quantitative data analysis of the MS raw-data, both Mascot and Sequest algorithms were used to identify protein-protein interactions in this study. The networks revealed very similar cellular processes for the two cell lines. In general, more proteins were detected in HEK293 cells compared to MKN45 cells. This might reflect the capability of

HEK293 cells to generate functional mature proteins [70]. Cancer cells express a different set of proteins compared to normal cells, especially alteration in cell-surface proteins and the nuclear proteomes [83]. Taken together, we did not expect to find all of the same proteins in the two cell lines. Further, our proteomic analyses need to be repeated to examine the reproducibility of the binding partners, and the proteins detected must be verified by other *in vitro* experiments.

In general, the annotations of the protein-protein networks were broad and the functional analysis gave a myriad of functions. This suggests that NR4A2 has an active role in many different biological processes. These include associating with proteins in the cytoskeleton, in cell signalling cascades, as well as proteins regulating transcription, post-transcriptional modifications, translation and DNA repair. The role of NR4A2 in regulation of these processes is poorly described up to date. The networks generated in this thesis should be regarded as a starting point for further investigation both to put forward hypotheses and to identify important cellular processes. The NR4A receptors have been shown to play essential roles in development and cellular homeostasis [28]. Our annotated networks included cellular development, cell morphology, cellular assembly and organization and are highly reliable since these biological functions are confirmed for NR4A2 in other studies. NR4A2 has been identified as an important factor in maintenance and development of the dopaminergic neurones in the brain [84], and mice lacking the NR4A2 expression die shortly after birth [85]. Mutations in NR4A2 are associated with neurodegenerative disorders like Parkinson [86, 87] and may be involved in the pathogenesis of schizophrenia [88, 89].

The proteomic results included proteins already published to bind to NR4A2 e.g. splicing factor, proline- and glutamine-rich (SFPQ) [90] and Poly [ADP-ribose] polymerase 1 (PARP-1) [91, 92]. However, these proteins had a low abundance in our experiment and did not make the decided cut-off of $\log_2$ ratio ≥ 0.58. PARP-1 has been shown to bind NR4A2 upon exposure to DNA damage, and translocate to the double-strand break foci where NR4A2 promotes double-strand break repair [92]. PARP-1 is also essential for NR4A2 recruitment to UV induced foci where it is involved in nucleotide excision repair [91]. Collectively, these studies may suggest a cell survival role for NR4A2. Interestingly, our results showed that the DNA

mismatch repair protein msh6 (MSH6) could bind to NR4A2. Further studies should be conducted to investigate whether NR4A2 binds to other DNA repair proteins and by this play a role in DNA repair.

Plasminogen activator inhibitor 1 RNA-binding protein (SERBP1) is a binding protein of plasminogen activator inhibitor 1 (PAI-1) mRNA and regulates the mRNA stability [93]. Our data suggest interactions of NR4A2 and SERBP1, which may indicate that NR4A2 can be part of the SERBP1 regulation complex. PAI-1 is a part of the urokinase plasminogen activator (uPA) system that is involved in degradation of basement membrane and the extracellular matrix that leads to cell invasion and metastasis [94]. Expression of PAI-1 and uPA is associated with poor prognosis in various cancers, including gastric cancer [95-97]. Previous studies in our research group have shown that gastrin induces the protein expression of PAI-1. Knock-down of PAI-1 increased gastrin mediated invasion and migration in the AGS-G_R cells, suggesting that PAI-1 plays an important role in restraining the effect of gastrin on cell motility [97]. Notably, when NR4A2 is knocked-down in the AGS-G_R cells an increase in the migration was observed [51], thus we speculate that NR4A2 may participate in stabilizing of PAI-1. The mechanisms controlling the expression and the role of PAI-1 in the gastric cancer is not fully understood, and further studies to characterize the function of NR4A2 and PAI-1 in gastric cancer would be highly interesting.

The Wnt-signalling pathway is central in the regulation of cell proliferation, migration and differentiation, and is often deregulated in gastric cancer [64, 65]. In absence of Wnt β catenin is regulated by a complex of Adenomatous polyposis coli (APC), Axin and GSK3β. Binding of Wnt-proteins to its receptor Frizzled and co-receptors low-density lipoprotein receptor-related protein 5/6 (LPR 5/6), subsequently blocks the phosphorylation and degradation of β-catenin [66, 98]. The results from our IP experiment showed that NR4A2 did not bind β–catenin in either MKN45 (figure 3.9) or HEK293 cells (figure 3.10). However, cross-talk between all NR4A receptors and β–catenin signalling pathway has been shown in the osteoblastic cell line U2-OS [72].

Several proteins in the Wnt-signalling pathway were detected to bind to NR4A2 by the proteomic approach. Microtubule-actin cross-linking factor 1 (MACF1) is a

positive regulator of the Wnt-signalling pathway, known to interact with Axin and involves the translocation of the Axin-complex to the LRP 5/6 at the cell membrane resulting in β–catenin accumulation [99]. A recent study found that 4/30 diffuse-type gastric carcinomas possess mutations in the *MACF1* gene [100]. Two receptors in the Wnt-signalling pathway were also detected, Frizzled-10 (FZD10) and Leucine-rich repeat-containing G-protein coupled receptor 4 (LGR4) [101, 102], and both proteins have been reported to be up-regulated in gastric intestinal cancer [102, 103]. Altogether these findings indicate that NR4A2 may modulate the Wnt-signalling pathway in at least two ways, either by directly binding the receptors or by regulating the translocation of the β-catenin complex to the receptors. Zagani *et al.* [49] has shown that blockage of NR4A2 and simultaneously inhibition of the Wnt/β-catenin signalling reduced tumor growth *in vivo* [49]. Interactions between NR4A2 and proteins in the Wnt-signalling pathway should be further explored.

NR4A2 has been shown to promote cell survival by interacting with p53 and repress the induction of pro-apoptotic genes [104]. Noteworthy, p53 is an important regulator of autophagy [105, 106]. Bouzas-Rodriguez *et al.* [107] have shown that NR4A1 can promote autophagy-mediated cell death. A fraction of the NR4A1 receptors were located in the cytoplasm, and shown to interact with p53. The mechanisms to promote cell death may involve protein-protein interaction as well as regulation of gene-expression of pro-autophagy genes. Interestingly, although this study refer to NR4A1, they did not rule out the possibility that NR4A2 could play a role in autophagy [107].

Serine/threonine-protein kinase STK11 (STK11) is often mutated in cancer [108, 109]. Germ line mutations in STK11 are responsible for Peutz-Jeghers syndrome and these patients have an increased risk of developing cancer, especially gastrointestinal cancers [109]. STK11 phosphorylates and activates at least 14 protein kinases and regulates cellular processes like cell division, cell growth and energy metabolism [110]. STK11 phosphorylates the AMP-activated protein kinase (AMPK) that regulates glucose and lipid metabolism in response to changes in intracellular energy level and nutrients [111]. The group has preliminary data showing that gastrin phosphorylates STK11-AMPK-ULK pathway and initiates autophagy, which may in part regulate the anti-apoptotic effect of gastrin (manuscript in preparation). The interaction between the NR4A receptors and STK11 is not fully understood. NR4A1

has been shown to sequester STK11 in the nucleus and hinder its cytoplasmic translocation and subsequently phosphorylation of AMPK [112]. Taken together, STK11 is found to be an interesting candidate protein for future work to generate new hypothesis regarding the role of both NR4A2 and STK11 in gastric cancer.

Some considerations regarding the experimental setup in this study need to be discussed. The preliminary results (figure 3.19) showed that the interaction between NR4A2 and STK11 could not be confirmed by Western blot, which underscore that further experiments and optimization is needed. For IP; the stringency of the washing buffer is essential to obtain a pure sample of the antigen and the antigen-binding partners. In the MS data, STK11 was detected only in the EGFP-NR4A2 sample of untreated MKN45 cells, however by the Western blot we detected binding of both EGFP-NR4A2 and EGFP. To investigate the interaction between NR4A2 and STK11, and optimize the IP and further, a dilution series of different concentrations of KCl in the washing buffer could be performed. If the protein dissociates at a lower salt concentration from EGFP compared to EGFP-NR4A2, this would reveal a stronger binding between NR4A2 and STK11, which confirms their interaction. The non-specific band at 50-55 kDa is most likely the heavy chain of IgG. The antibody used to immunoprecipitate was rabbit, thus it would be better to use an antibody from a different species when blotting for STK11.

Protein-protein interactions are essential for almost every process in a living cell. Multi-protein complexes are involved in the regulation of many biological processes, and the majority of proteins are dependent on protein interactions for proper activity. The protein-protein interactions are highly dynamic and regulated by particular signals and the specific status of the cell [113]. In this study, we have identified putative protein-protein interactions of NR4A2, which uncover the versatile role of NR4A2. The study has provided ideas about the molecular mechanisms where NR4A2 may play a dual role, which may determine the cellular phenotype. Further investigation is needed to unravel whether gastrin regulates NR4A2 dependent cellular functions. As NR4A2 has been suggested to be a prognostic marker in gastric cancer. A better understanding of the molecular mechanisms involving NR4A2 is important to further uncover its role in cancer therapy.

References

1. Ferlay, J., et al., *Estimates of worldwide burden of cancer in 2008: GLOBOCAN 2008.* International Journal of Cancer, 2010. **127**(12): p. 2893-2917.
2. Crew, K.D. and A.I. Neugut, *Epidemiology of gastric cancer.* World J Gastroenterol, 2006. **12**(3): p. 354-62.
3. Dikken, J.L., et al., *Treatment of resectable gastric cancer.* Therap Adv Gastroenterol, 2012. **5**(1): p. 49-69.
4. Power, D.G., D.P. Kelsen, and M.A. Shah, *Advanced gastric cancer--slow but steady progress.* Cancer Treat Rev, 2010. **36**(5): p. 384-92.
5. Milne, A.N., et al., *Nature meets nurture: molecular genetics of gastric cancer.* Hum Genet, 2009. **126**(5): p. 615-28.
6. Hu, B., et al., *Gastric cancer: Classification, histology and application of molecular pathology.* J Gastrointest Oncol, 2012. **3**(3): p. 251-61.
7. Burkitt, M.D., A. Varro, and D.M. Pritchard, *Importance of gastrin in the pathogenesis and treatment of gastric tumors.* World J Gastroenterol, 2009. **15**(1): p. 1-16.
8. Resende, C., A. Ristimaki, and J.C. Machado, *Genetic and epigenetic alteration in gastric carcinogenesis.* Helicobacter, 2010. **15 Suppl 1**: p. 34-9.
9. Edkins, J.S., *The chemical mechanism of gastric secretion.* J Physiol, 1906. **34**(1-2): p. 133-44.
10. Dimaline, R. and A. Varro, *Attack and defence in the gastric epithelium - a delicate balance.* Exp Physiol, 2007. **92**(4): p. 591-601.
11. Ferrand, A. and T.C. Wang, *Gastrin and cancer: a review.* Cancer Lett, 2006. **238**(1): p. 15-29.
12. Dufresne, M., C. Seva, and D. Fourmy, *Cholecystokinin and gastrin receptors.* Physiol Rev, 2006. **86**(3): p. 805-47.
13. Watson, S.A., et al., *Gastrin - active participant or bystander in gastric carcinogenesis?* Nat Rev Cancer, 2006. **6**(12): p. 936-46.
14. Mills, J.C. and R.A. Shivdasani, *Gastric epithelial stem cells.* Gastroenterology, 2011. **140**(2): p. 412-24.
15. Koh, T.J., et al., *Gastrin deficiency results in altered gastric differentiation and decreased colonic proliferation in mice.* Gastroenterology, 1997. **113**(3): p. 1015-25.
16. Friis-Hansen, L., et al., *Impaired gastric acid secretion in gastrin-deficient mice.* Am J Physiol, 1998. **274**(3 Pt 1): p. G561-8.
17. Rai, R., et al., *Cholecystokinin and gastrin receptors targeting in gastrointestinal cancer.* Surg Oncol, 2012. **21**(4): p. 281-92.
18. Chen, D.A., et al., *Differentiation of gastric ECL cells is altered in CCK2 receptor-deficient mice.* Gastroenterology, 2002. **123**(2): p. 577-585.
19. Wang, T.C., et al., *Synergistic interaction between hypergastrinemia and Helicobacter infection in a mouse model of gastric cancer.* Gastroenterology, 2000. **118**(1): p. 36-47.
20. Dockray, G., R. Dimaline, and A. Varro, *Gastrin: old hormone, new functions.* Pflugers Arch, 2005. **449**(4): p. 344-55.

21. Roosenburg, S., et al., *Radiolabeled CCK/gastrin peptides for imaging and therapy of CCK2 receptor-expressing tumors.* Amino Acids, 2011. **41**(5): p. 1049-58.
22. Henwood, M., et al., *Expression of gastrin in developing gastric adenocarcinoma.* Br J Surg, 2001. **88**(4): p. 564-8.
23. Hur, K., et al., *Expression of gastrin and its receptor in human gastric cancer tissues.* J Cancer Res Clin Oncol, 2006. **132**(2): p. 85-91.
24. Willard, M.D., et al., *Somatic mutations in CCK2R alter receptor activity that promote oncogenic phenotypes.* Mol Cancer Res, 2012. **10**(6): p. 739-49.
25. Grabowska, A.M. and S.A. Watson, *Role of gastrin peptides in carcinogenesis.* Cancer Lett, 2007. **257**(1): p. 1-15.
26. Selvik, L.K., et al., *The duration of gastrin treatment affects global gene expression and molecular responses involved in ER stress and anti-apoptosis.* BMC Genomics, 2013. **14**: p. 429.
27. Maxwell, M.A. and G.E. Muscat, *The NR4A subgroup: immediate early response genes with pleiotropic physiological roles.* Nucl Recept Signal, 2006. **4**: p. e002.
28. Safe, S., et al., *Minireview: role of orphan nuclear receptors in cancer and potential as drug targets.* Mol Endocrinol, 2014. **28**(2): p. 157-72.
29. Han, Y., et al., *Expression of orphan nuclear receptor NR4A2 in gastric cancer cells confers chemoresistance and predicts an unfavorable postoperative survival of gastric cancer patients with chemotherapy.* Cancer, 2013. **119**(19): p. 3436-45.
30. Inamoto, T., et al., *Cytoplasmic Mislocalization of the Orphan Nuclear Receptor Nurr1 Is a Prognostic Factor in Bladder Cancer.* Cancer, 2010. **116**(2): p. 340-346.
31. Wang, J., et al., *Orphan Nuclear Receptor Nurr1 as a Potential Novel Marker for Progression in Human Prostate Cancer.* Asian Pacific Journal of Cancer Prevention, 2013. **14**(3): p. 2023-2028.
32. Llopis, S., et al., *Dichotomous roles for the orphan nuclear receptor NURR1 in breast cancer.* BMC Cancer, 2013. **13**: p. 139.
33. Han, Y.F. and G.W. Cao, *Role of nuclear receptor NR4A2 in gastrointestinal inflammation and cancers.* World J Gastroenterol, 2012. **18**(47): p. 6865-73.
34. Han, Y., et al., *Nuclear orphan receptor NR4A2 confers chemoresistance and predicts unfavorable prognosis of colorectal carcinoma patients who received postoperative chemotherapy.* Eur J Cancer, 2013. **49**(16): p. 3420-30.
35. Zhao, Y. and D. Bruemmer, *NR4A orphan nuclear receptors: transcriptional regulators of gene expression in metabolism and vascular biology.* Arterioscler Thromb Vasc Biol, 2010. **30**(8): p. 1535-41.
36. Pearen, M.A. and G.E. Muscat, *Minireview: Nuclear hormone receptor 4A signaling: implications for metabolic disease.* Mol Endocrinol, 2010. **24**(10): p. 1891-903.
37. Glass, C.K. and M.G. Rosenfeld, *The coregulator exchange in transcriptional functions of nuclear receptors.* Genes Dev, 2000. **14**(2): p. 121-41.
38. Safe, S., et al., *NR4A orphan receptors and cancer* Nuclear Receptor Signaling, 2011. **9**: p. e002.

39. Decressac, M., et al., *NURR1 in Parkinson disease--from pathogenesis to therapeutic potential.* Nat Rev Neurol, 2013. **9**(11): p. 629-36.
40. Shi, Y., *Orphan nuclear receptors in drug discovery.* Drug Discov Today, 2007. **12**(11-12): p. 440-5.
41. Wang, Z., et al., *Structure and function of Nurr1 identifies a class of ligand-independent nuclear receptors.* Nature, 2003. **423**(6939): p. 555-60.
42. Sacchetti, P., et al., *Multiple signaling pathways regulate the transcriptional activity of the orphan nuclear receptor NURR1.* Nucleic Acids Res, 2006. **34**(19): p. 5515-27.
43. Arredondo, C., et al., *PIASgamma enhanced SUMO-2 modification of Nurr1 activation-function-1 domain limits Nurr1 transcriptional synergy.* PLoS One, 2013. **8**(1): p. e55035.
44. Jo, A.Y., et al., *Generation of dopamine neurons with improved cell survival and phenotype maintenance using a degradation-resistant nurr1 mutant.* Stem Cells, 2009. **27**(9): p. 2238-46.
45. Baek, S.H. and M.G. Rosenfeld, *Nuclear receptor coregulators: their modification codes and regulatory mechanism by translocation.* Biochemical and Biophysical Research Communications, 2004. **319**(3): p. 707-714.
46. Garcia-Yague, A.J., et al., *Nuclear import and export signals control the subcellular localization of Nurr1 protein in response to oxidative stress.* J Biol Chem, 2013. **288**(8): p. 5506-17.
47. Mohan, H.M., et al., *Molecular pathways: the role of NR4A orphan nuclear receptors in cancer.* Clin Cancer Res, 2012. **18**(12): p. 3223-8.
48. Holla, V.R., et al., *Prostaglandin E2 regulates the nuclear receptor NR4A2 in colorectal cancer.* J Biol Chem, 2006. **281**(5): p. 2676-82.
49. Zagani, R., et al., *Cyclooxygenase-2 inhibitors down-regulate osteopontin and Nr4A2-new therapeutic targets for colorectal cancers.* Gastroenterology, 2009. **137**(4): p. 1358-66 e1-3.
50. Chang, W.J., et al., *Identification of novel hub genes associated with liver metastasis of gastric cancer.* International Journal of Cancer, 2009. **125**(12): p. 2844-2853.
51. Misund, K., et al., *NR4A2 is regulated by gastrin and influences cellular responses of gastric adenocarcinoma cells.* PLoS One, 2013. **8**(9): p. e76234.
52. Lal, A., S.R. Haynes, and M. Gorospe, *Clean Western blot signals from immunoprecipitated samples.* Mol Cell Probes, 2005. **19**(6): p. 385-8.
53. Dagda, R.K., T. Sultana, and J. Lyons-Weiler, *Evaluation of the Consensus of Four Peptide Identification Algorithms for Tandem Mass Spectrometry Based Proteomics.* J Proteomics Bioinform, 2010. **3**: p. 39-47.
54. Livak, K.J. and T.D. Schmittgen, *Analysis of relative gene expression data using real-time quantitative PCR and the 2(-Delta Delta C(T)) Method.* Methods, 2001. **25**(4): p. 402-8.
55. Riss, T.L., et al., *Cell Viability Assays*, in *Assay Guidance Manual*, G.S. Sittampalam, et al., Editors. 2004: Bethesda (MD).
56. McWilliams, D.F., et al., *Coexpression of gastrin and gastrin receptors (CCK-B and delta CCK-B) in gastrointestinal tumour cell lines.* Gut, 1998. **42**(6): p. 795-8.

57. Konturek, P.C., et al., *Influence of gastrin on the expression of cyclooxygenase-2, hepatocyte growth factor and apoptosis-related proteins in gastric epithelial cells.* J Physiol Pharmacol, 2003. **54**(1): p. 17-32.
58. Watson, S., L. Durrant, and D. Morris, *Gastrin: growth enhancing effects on human gastric and colonic tumour cells.* Br J Cancer, 1989. **59**(4): p. 554-8.
59. Watson, S.A., et al., *Therapeutic effect of the gastrin receptor antagonist, CR2093 on gastrointestinal tumour cell growth.* Br J Cancer, 1992. **65**(6): p. 879-83.
60. Sun, W.H., et al., *Blockade of cholecystokinin-2 receptor and cyclooxygenase-2 synergistically induces cell apoptosis, and inhibits the proliferation of human gastric cancer cells in vitro.* Cancer Lett, 2008. **263**(2): p. 302-11.
61. Watson, F., et al., *Transcriptional activation of the rat vesicular monoamine transporter 2 promoter in gastric epithelial cells: regulation by gastrin.* J Biol Chem, 2001. **276**(10): p. 7661-71.
62. Ashurst, H.L., A. Varro, and R. Dimaline, *Regulation of mammalian gastrin/CCK receptor (CCK2R) expression in vitro and in vivo.* Exp Physiol, 2008. **93**(2): p. 223-36.
63. Mix, K.S., et al., *Transcriptional repression of matrix metalloproteinase gene expression by the orphan nuclear receptor NURR1 in cartilage.* J Biol Chem, 2007. **282**(13): p. 9492-504.
64. Clements, W.M., et al., *beta-Catenin mutation is a frequent cause of Wnt pathway activation in gastric cancer.* Cancer Res, 2002. **62**(12): p. 3503-6.
65. Katoh, M., et al., *WNT2B2 mRNA, up-regulated in primary gastric cancer, is a positive regulator of the WNT- beta-catenin-TCF signaling pathway.* Biochem Biophys Res Commun, 2001. **289**(5): p. 1093-8.
66. Mulholland, D.J., et al., *Interaction of nuclear receptors with the Wnt/beta-catenin/Tcf signaling axis: Wnt you like to know?* Endocr Rev, 2005. **26**(7): p. 898-915.
67. Pradeep, A., et al., *Gastrin-mediated activation of cyclin D1 transcription involves beta-catenin and CREB pathways in gastric cancer cells.* Oncogene, 2004. **23**(20): p. 3689-99.
68. Hocker, M., et al., *Sp1 and CREB mediate gastrin-dependent regulation of chromogranin A promoter activity in gastric carcinoma cells.* J Biol Chem, 1998. **273**(51): p. 34000-7.
69. Conkright, M.D., et al., *TORCs: transducers of regulated CREB activity.* Mol Cell, 2003. **12**(2): p. 413-23.
70. Thomas, P. and T.G. Smart, *HEK293 cell line: a vehicle for the expression of recombinant proteins.* J Pharmacol Toxicol Methods, 2005. **51**(3): p. 187-200.
71. Kitagawa, H., et al., *A Regulatory Circuit Mediating Convergence between Nurr1 Transcriptional Regulation and Wnt Signaling (Retraction of vol 27, pg 7486, 2007).* Molecular and Cellular Biology, 2014. **34**(5): p. 917-917.
72. Rajalin, A.M. and P. Aarnisalo, *Cross-talk between NR4A orphan nuclear receptors and beta-catenin signaling pathway in osteoblasts.* Arch Biochem Biophys, 2011. **509**(1): p. 44-51.
73. Wu, Q., et al., *Downregulation of RPL6 by siRNA inhibits proliferation and cell cycle progression of human gastric cancer cell lines.* PLoS One, 2011. **6**(10): p. e26401.

74. Rybakin, V. and C.S. Clemen, *Coronin proteins as multifunctional regulators of the cytoskeleton and membrane trafficking.* Bioessays, 2005. **27**(6): p. 625-632.
75. Mannini, L., et al., *Spectrum and consequences of SMC1A mutations: the unexpected involvement of a core component of cohesin in human disease.* Hum Mutat, 2010. **31**(1): p. 5-10.
76. Lin, Q., et al., *iTRAQ analysis of colorectal cancer cell lines suggests Drebrin (DBN1) is overexpressed during liver metastasis.* Proteomics, 2014.
77. Boldingh Debernard, K.A., G.H. Mathisen, and R.E. Paulsen, *Differences in NGFI-B, Nurr1, and NOR-1 expression and nucleocytoplasmic translocation in glutamate-treated neurons.* Neurochem Int, 2012. **61**(1): p. 79-88.
78. Satoh, J. and Y. Kuroda, *The constitutive and inducible expression of Nurr1, a key regulator of dopaminergic neuronal differentiation, in human neural and non-neural cell lines.* Neuropathology, 2002. **22**(4): p. 219-32.
79. Volakakis, N., et al., *NR4A orphan nuclear receptors as mediators of CREB-dependent neuroprotection.* Proceedings of the National Academy of Sciences of the United States of America, 2010. **107**(27): p. 12317-12322.
80. Thompson, J., et al., *Protein kinase C regulates mitochondrial targeting of Nur77 and its family member Nor-1 in thymocytes undergoing apoptosis.* Eur J Immunol, 2010. **40**(7): p. 2041-9.
81. Lin, B., et al., *Conversion of Bcl-2 from protector to killer by interaction with nuclear orphan receptor Nur77/TR3.* Cell, 2004. **116**(4): p. 527-40.
82. ten Have, S., et al., *Mass spectrometry-based immuno-precipitation proteomics - the user's guide.* Proteomics, 2011. **11**(6): p. 1153-9.
83. Wisniewski, J.R., et al., *Extensive quantitative remodeling of the proteome between normal colon tissue and adenocarcinoma.* Mol Syst Biol, 2012. **8**: p. 611.
84. Kadkhodaei, B., et al., *Nurr1 Is Required for Maintenance of Maturing and Adult Midbrain Dopamine Neurons.* Journal of Neuroscience, 2009. **29**(50): p. 15923-15932.
85. Zetterstrom, R.H., et al., *Dopamine neuron agenesis in Nurr1-deficient mice.* Science, 1997. **276**(5310): p. 248-50.
86. Liu, H., et al., *Genetic analysis of NR4A2 gene in a large population of Han Chinese patients with Parkinson's disease.* Eur J Neurol, 2013. **20**(3): p. 584-7.
87. Sleiman, P.M., et al., *Characterisation of a novel NR4A2 mutation in Parkinson's disease brain.* Neurosci Lett, 2009. **457**(2): p. 75-9.
88. Chen, Y.H., et al., *Mutation analysis of the human NR4A2 gene, an essential gene for midbrain dopaminergic neurogenesis, in schizophrenic patients.* Am J Med Genet, 2001. **105**(8): p. 753-7.
89. Ancin, I., et al., *NR4A2: effects of an "orphan" receptor on sustained attention in a schizophrenic population.* Schizophr Bull, 2013. **39**(3): p. 555-63.
90. Jacobs, F.M., et al., *Pitx3 potentiates Nurr1 in dopamine neuron terminal differentiation through release of SMRT-mediated repression.* Development, 2009. **136**(4): p. 531-40.
91. Jagirdar, K., et al., *The NR4A2 Nuclear Receptor Is Recruited to Novel Nuclear Foci in Response to UV Irradiation and Participates in Nucleotide Excision Repair.* Plos One, 2013. **8**(11).

92. Malewicz, M., et al., *Essential role for DNA-PK-mediated phosphorylation of NR4A nuclear orphan receptors in DNA double-strand break repair.* Genes Dev, 2011. **25**(19): p. 2031-40.
93. Heaton, J.H., et al., *Identification and cDNA cloning of a novel RNA-binding protein that interacts with the cyclic nucleotide-responsive sequence in the type-1 plasminogen activator inhibitor mRNA.* Journal of Biological Chemistry, 2001. **276**(5): p. 3341-3347.
94. Dass, K., et al., *Evolving role of uPA/uPAR system in human cancers.* Cancer Treat Rev, 2008. **34**(2): p. 122-36.
95. Durand, M.K., et al., *Plasminogen activator inhibitor-1 and tumour growth, invasion, and metastasis.* Thrombosis and Haemostasis, 2004. **91**(3): p. 438-449.
96. Beyer, B.C.M., et al., *Urokinase system expression in gastric carcinoma - Prognostic impact in an independent patient series and first evidence of predictive value in preoperative biopsy and intestinal metaplasia specimens.* Cancer, 2006. **106**(5): p. 1026-1035.
97. Norsett, K.G., et al., *Gastrin stimulates expression of plasminogen activator inhibitor-1 in gastric epithelial cells.* Am J Physiol Gastrointest Liver Physiol, 2011. **301**(3): p. G446-53.
98. Polakis, P., *The many ways of Wnt in cancer.* Curr Opin Genet Dev, 2007. **17**(1): p. 45-51.
99. Chen, H.J., et al., *The role of microtubule actin cross-linking factor 1 (MACF1) in the Wnt signaling pathway.* Genes Dev, 2006. **20**(14): p. 1933-45.
100. Kakiuchi, M., et al., *Recurrent gain-of-function mutations of RHOA in diffuse-type gastric carcinoma.* Nat Genet, 2014.
101. Glinka, A., et al., *LGR4 and LGR5 are R-spondin receptors mediating Wnt/beta-catenin and Wnt/PCP signalling.* EMBO Rep, 2011. **12**(10): p. 1055-61.
102. Terasaki, H., et al., *Frizzled-10, up-regulated in primary colorectal cancer, is a positive regulator of the WNT - beta-catenin - TCF signaling pathway.* Int J Mol Med, 2002. **9**(2): p. 107-12.
103. Steffen, J.S., et al., *LGR4 and LGR6 are differentially expressed and of putative tumor biological significance in gastric carcinoma.* Virchows Arch, 2012. **461**(4): p. 355-65.
104. Zhang, T., et al., *NGFI-B nuclear orphan receptor Nurr1 interacts with p53 and suppresses its transcriptional activity.* Mol Cancer Res, 2009. **7**(8): p. 1408-15.
105. Tasdemir, E., et al., *A dual role of p53 in the control of autophagy.* Autophagy, 2008. **4**(6): p. 810-814.
106. Brady, C.A. and L.D. Attardi, *p53 at a glance.* Journal of Cell Science, 2010. **123**(15): p. 2527-2532.
107. Bouzas-Rodriguez, J., et al., *The nuclear receptor NR4A1 induces a form of cell death dependent on autophagy in mammalian cells.* PLoS One, 2012. **7**(10): p. e46422.
108. Hezel, A.F. and N. Bardeesy, *LKB1; linking cell structure and tumor suppression.* Oncogene, 2008. **27**(55): p. 6908-19.
109. Katajisto, P., et al., *The LKB1 tumor suppressor kinase in human disease.* Biochim Biophys Acta, 2007. **1775**(1): p. 63-75.

110. Vaahtomeri, K. and T.P. Makela, *Molecular mechanisms of tumor suppression by LKB1.* Febs Letters, 2011. **585**(7): p. 944-951.
111. Shackelford, D.B. and R.J. Shaw, *The LKB1-AMPK pathway: metabolism and growth control in tumour suppression.* Nat Rev Cancer, 2009. **9**(8): p. 563-75.
112. Zhan, Y.Y., et al., *The orphan nuclear receptor Nur77 regulates LKB1 localization and activates AMPK.* Nat Chem Biol, 2012. **8**(11): p. 897-904.
113. Ngounou Wetie, A.G., et al., *Protein-protein interactions: switch from classical methods to proteomics and bioinformatics-based approaches.* Cell Mol Life Sci, 2014. **71**(2): p. 205-28.

Appendix

Appendix 1

The EGFP-NR4A2 plasmid, shown in figure A1.1.

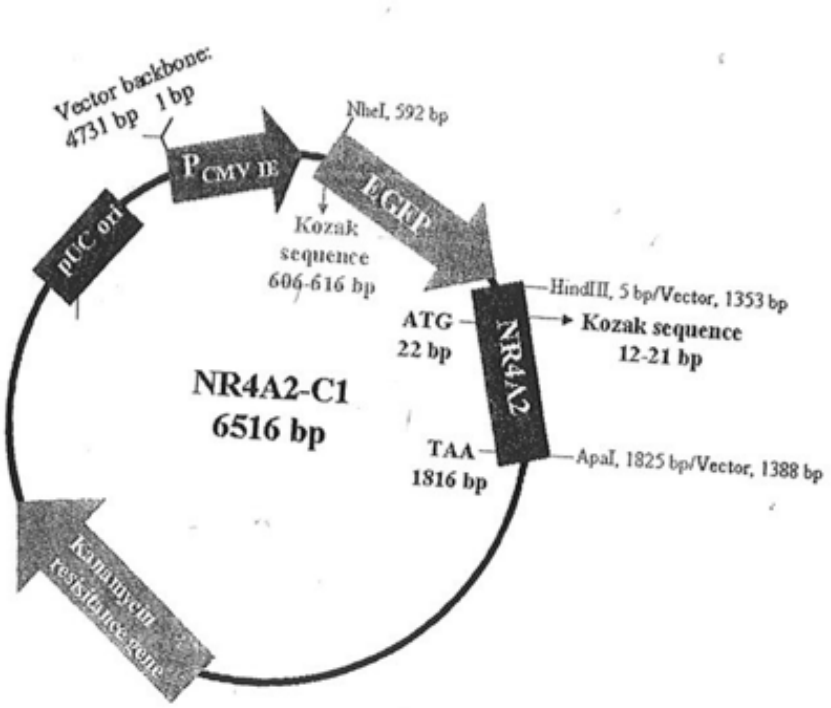

Figure A1.1. EGFP-NR4A2 plasmid.

Appendix 2

A melt curve analysis was performed, and shown in figure A2.1.

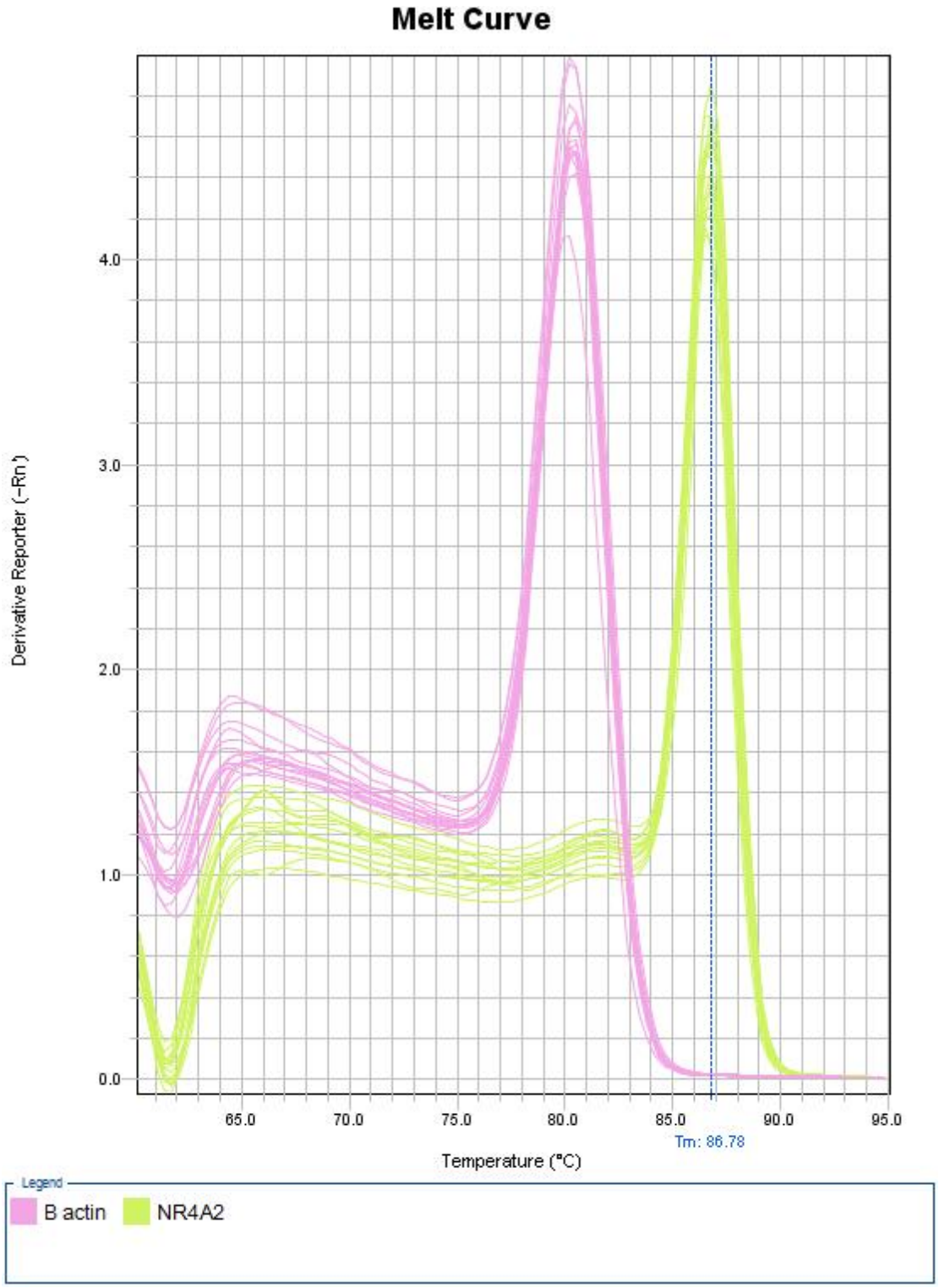

Figure A2.1. **The melt curve of the PCR products.** The melt curve shows the melt curve of β-actin in pink, and NR4A2 in green. The data represent one of two biological experiments.

Appendix 3

HEK293 and MKN45 were seeded in 96-well plates and cultivated for 24 hours. The cells were then transfected with 0.1µg plasmid and 0.5 µl Metafectene PRO/ well. The MTT analysis was performed 48 hours after transfection.

No statistical significance (p-value ≤0.05) between the transfected cells was identified using a two-tailed independent Student´s t-test.

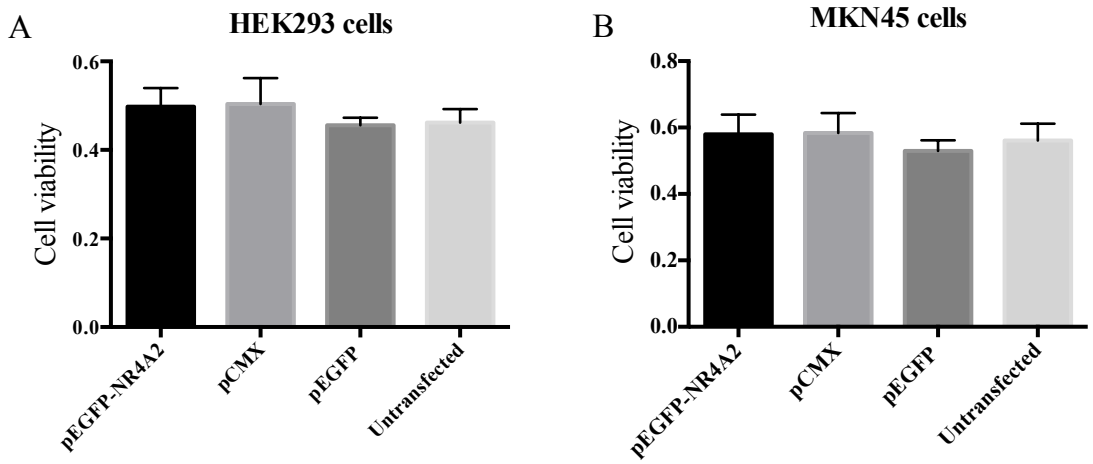

Figure A3.1. **Viability assay of transfected cells.** HEK293 cells and MKN45 (A and B, respectively) were transfected with the plasmids indicated. Transfection of the cells does not affect the viability of the cells significantly (p-value ≤ 0.05). The data shown is mean ± SD.

Appendix 4

Ingenuity Pathway Analysis was used to generate networks of the proteins detected after Mass Spectrometry of the immunoprecipitated samples. The detection cut-off in IPA was decided to be $\log_2$ ratio ≥ 0.58. The complete lists of potential interacting partners of NR4A2 in untreated MKN45 cells (table A4.1), gastrin (30 minutes) treated cells (table A4.2) and HEK293 (table A4.3) are presented.

Table A4.1. The proteins detected in US MKN45 cells

Mascot	**Gene symbol**	**Log_2 value**
Myosin-VI (Unconventional myosin VI)	MYO6	6,320
Ankyrin-3	ANK3	5,515
Tripartite motif-containing protein 58	TRIM58	5,424
Serine/threonine-protein kinase STK11	STK11	5,319
Putative pre-mRNA-splicing factor ATP-dependent RNA helicase DHX16	DHX16	5,065
Protein phosphatase 1 regulatory subunit 12A	PPP1R12A	4,971
Polypyrimidine tract-binding protein 3	ROD1	4,866
60S ribosomal protein L6	RPL6	4,832
Polyadenylate-binding protein 4	PABPC4	4,612
PRAME family member 9	PRAMEF9	4,526
Muscarinic acetylcholine receptor M3	CHRM3	4,525
Sequest	**Gene symbol**	**Log_2 value**
Isoform 5 of E3 ubiquitin-protein ligase	UBR4	1,784
Tetratricopeptide repeat protein 23 (fragment)	TTC23	1,722
Isoform 2 of EF-hand calcium-binding domain-containing protein 4A	EFCAB4A	1,642
Low-density lipoprotein receptor-related protein 1B (fragment)	LRP1B	1,611
Transmembrane protein PVRIG	PVRIG	1,597
60S ribosomal protein L4 (Fragment)	RPL4	1,547
Isoform 2 of Tudor domain-containing protein 6	TDRD6	1,540
Ubiquitin carboxyl-terminal hydrolase	USP24	1,472
Isoform 4 of Dynein heavy chain 17, axonemal	DNAH17	1,186
Nuclear pore complex-interacting protein family member A2	NPIPA2	1,163
Zinc finger protein 423	ZNF423	1,129
Microtubule-associated serine/threonine-protein kinase 2	MAST2	1,077
Secreted glypican-3 (Fragment)	GPC3	0,884
Gem-associated protein 4	GEMIN4	0,751
Isoform 2 of Leucine-rich repeat-containing G-protein coupled receptor 4	LGR4	0,720
Isoform 11 of Histone deacetylase 9	HDAC9	0,687

Table A4.2. The proteins detected in MKN45 cells stimulated with gastrin (10 nM) for 30 minutes

Mascot	**Gene symbol**	**Log_2 value**
Protein phosphatase 1 regulatory subunit 12C	PPP1R12C	5,478
Cytosolic phospholipase A2 beta	PLA2G4B	5,310
60S ribosomal protein L6	RPL6	5,210
Exosome complex component MTR3	EXOSC6	5,154
Interferon-induced GTP-binding protein Mx1	MX1	4,924
60S ribosomal protein L13	RPL13	4,579
Frizzled-10	FZD10	4,539
Sequest	**Gene symbol**	**Log_2 value**
Isoform 2 of 26S proteasome non-ATPase regulatory subunit 11	PSMD11	2,226
Synaptotagmin-like protein 1	SYTL1	1,690
Polycystic kidney disease 2-like 1 protein (Fragment)	PKD2L1	0,714
N6-adenosine-methyltransferase 70 kDa subunit	METTL3	0,687

Table A4.3. The proteins detected in HEK293 cells

Mascot	Gene symbol	Log_2 value
Actin-binding protein anillin	ANLN	5,808
Multiple myeloma tumor-associated protein 2	MMTAG2	5,523
Drebrin	DBN1	5,463
40S ribosomal protein S4, X isoform	RPS4X	5,454
Glutamine-rich protein 1	QRICH1	5,440
Coronin-1A	CORO1A	5,434
Desmoplakin	DSP	5,414
Splicing factor 3 subunit 1	SF3A1	5,346
Serine/threonine-protein phosphatase 2A regulatory subunit B" subunit alpha	PPP2R3A	5,322
Epiplakin	EPPK1	5,302
Proliferation-associated protein 2G4	PA2G4	5,224
T-complex protein 1 subunit beta	CCT2	5,223
40S ribosomal protein S3	RPS3	5,182
Transcription intermediary factor 1-beta	TRIM28	5,179
Dystonin	DST	5,179
RNA-binding motif protein, X chromosome	RBMX	5,085
60S ribosomal protein L6	RPL6	5,070
Coiled-coil domain-containing protein 124	CCDC124	5,067
Serine/threonine-protein phosphatase 2A catalytic subunit beta isoform	PPP2CB	5,042
60 kDa heat shock protein, mitochondrial	HSPD1	5,039
Coatomer subunit epsilon	COPE	4,976
Vasodilator-stimulated phosphoprotein	VASP	4,937
DNA mismatch repair protein Msh6	MSH6	4,925
40S ribosomal protein S16	RPS16	4,900
ATP-dependent RNA helicase DDX54	DDX54	4,842
Ubiquitin-activating enzyme E1	UBA1	4,822
Unconventional myosin-Id	MYO1D	4,729
Coronin-2A	CORO2A	4,631
Probable ATP-dependent RNA helicase DDX17	DDX17	4,599
Nipped-B-like protein	NIPBL	4,581
Mitochondrial import inner membrane translocase subunit TIM50	TIMM50	4,489
Splicing factor 45	RBM17	4,472
Polypyrimidine tract-binding protein 1	PTBP1	4,449
Delta 1-pyrroline-5-carboxylate synthase	ALDH18A1	4,391
Myosin phosphatase Rho-interacting protein	MPRIP	0,809
Structural maintenance of chromosomes protein 1A	SMC1A	0,630
DNA ligase 3	LIG3	0,615

Sequest	Gene symbol	Log_2 value
Plasminogen activator inhibitor 1 RNA-binding protein	SERBP1	2,844
Zinc finger CCHC domain-containing protein 3	ZCCHC3	2,066
Structural maintenance of chromosomes protein 1A	SMC1A	1,717
Drebrin-like protein	DBNL	1,658
Coronin-1C	CORO1C	1,652
Drebrin	DBN1	1,545
Isoform 2 of Leucine zipper protein 1	LUZP1	1,462
Nuclear pore membrane glycoprotein 210	NUP210	1,460
OTU domain-containing protein 7A	OTUD7A	1,417
Dynein heavy chain 10, axonemal	DNAH10	1,392
Olfactory receptor 3A3	OR3A3	1,297
Isoform 5 of Bifunctional UDP-N-acetylglucosamine 2-epimerase/ N-acetylmannosamine kinase	GNE	1,174
Mediator of RNA polymerase II transcription subunit 24	MED24	1,122
Spectrin alpha chain, non-erythrocytic 1	SPTAN1	1,108
Junction plakoglobin	JUP	1,065
Coronin-1A	CORO1A	1,062
Microtubule-actin cross-linking factor 1, isoforms 1/2/3/5	MACF1	0,956
Putative ATP-dependent RNA helicase DHX57	DHX57	0,942
POTE ankyrin domain family member E	POTEE	0,924
CTTNBP2 N-terminal-like protein	CTTNBP2NL	0,913
Kinesin-like protein KIF2C (Fragment)	KIF2C	0,900
Talin-1	TLN1	0,881
Uridine diphosphate glucose pyrophosphatase	NUDT14	0,880
ATP synthase subunit alpha, mitochondrial	ATP5A1	0,865
Polyubiquitin-C	UBC	0,858
Low-density lipoprotein receptor-related protein 5	LRP5	0,838
T-complex protein 1 subunit gamma (Fragment)	CCT3	0,797
Threonine--tRNA ligase, mitochondrial	TARS2	0,752
KH domain-containing, RNA-binding, signal transduction-associated protein 1	KHDRBS1	0,700
Glutamate dehydrogenase 1, mitochondrial	GLUD1	0,693
Protein phosphatase 1 regulatory subunit 12C	PPP1R12C	0,669

Appendix 5.

Ingenuity Pathway Analysis was used to generate networks of the proteins detected after Mass Spectrometry of the immunoprecipitated samples. The associated network functions of the protein of the networks not presented in the result-part of MKN45 cells detected by Sequest (table A5.1), HEK293 cells detected by Sequest (table A5.2) and Mascot (table A5.3) are presented.

Table A5.1. MKN45 cells untreated (Sequest)

Associated network functions	Number of proteins from the dataset	Score
RNA post-transcriptional modifications, cell cycle, cellular growth and proliferation	4	9
Cellular assembly and organization, cell cycle, cell death and survival	1	3

Table A5.2. HEK293 cells (Sequest)

Associated network functions	Number of proteins from the dataset	Score
Carbohydrate metabolism, Lipid metabolism, small molecule biochemistry	2	3
Hereditary disorder, respiratory disease, organismal injury and abnormalities	1	2

Table A5.3. HEK293 cells (Mascot)

Associated network functions	Number of proteins from the dataset	Score
Connective tissue disorders, dermatological diseases and conditions, developmental disorders	14	33